Silyl-Osmium(IV)-Trihydride Complexes Stabilized by a Pincer Ether-Diphosphine: Formation and Reactions with Alkynes

Juan C. Babón, Miguel A. Esteruelas, Enrique Oñate, Sonia Paz, and Andrea Vélez*

Departamento de Química Inorgánica – Instituto de Síntesis Química y Catálisis Homogénea (ISQCH) – Centro de Innovación en Química Avanzada (ORFEO-CINQA), Universidad de Zaragoza – CSIC, 50009 Zaragoza, Spain

ABSTRACT:

Complex $OsH_4\{\kappa^3\text{-}P,O,P\text{-}[xant(P^iPr_2)_2]\}$ (**1**) activates the Si–H bond of triethylsilane, triphenylsilane, and 1,1,1,3,5,5,5-heptamethyltrisiloxane to give the silyl-osmium(IV)-trihydride derivatives $OsH_3(SiR_3)\{\kappa^3\text{-}P,O,P\text{-}[xant(P^iPr_2)_2]\}$ (SiR_3 = $SiEt_3$ (**2**), $SiPh_3$ (**3**), $SiMe(OSiMe_3)_2$ (**4**)) and H_2. The activation takes place via an unsaturated tetrahydride intermediate, resulting from the dissociation of the oxygen atom of the pincer ligand 9,9-dimethyl-4,5-bis(diisopropylphosphino)xanthene ($xant(P^iPr_2)_2$). This intermediate, which has been trapped to form $OsH_4\{\kappa^2\text{-}P,P\text{-}[xant(P^iPr_2)_2]\}(P^iPr_3)$ (**5**), coordinates the Si–H bond of the silanes to subsequently undergo a homolytic cleavage. Kinetics of the reaction along with the observed

primary isotope effect demonstrate that the Si–H rupture is the rate determining step of the activation. Complex **2** reacts with 1,1-diphenyl-2-propyn-1-ol and 1-phenyl-1-propyne. The reaction with the former affords $Os\{C{\equiv}CC(OH)Ph_2\}_2\{{=}C{=}CHC(OH)Ph_2\}\{\kappa^3\text{-}P,O,P\text{-}[xant(P^iPr_2)_2]\}$ (**6**), which catalyzes the conversion of the propargylic alcohol into (*E*)-2-(5,5-diphenylfuran-2(*5H*)-ylidene)-1,1-diphenylethan-1-ol, via the (*Z*)-enynediol. In methanol, the hydroxyvinylidene ligand of **6** dehydrates to allenylidene, generating $Os\{C{\equiv}CC(OH)Ph_2\}_2\{{=}C{=}C{=}CPh_2\}\{\kappa^3\text{-}P,O,P\text{-}[xant(P^iPr_2)_2]\}$ (**7**). The reaction of **2** with 1-phenyl-1-propyne leads to $OsH\{\kappa^1\text{-}C,\eta^2\text{-}[C_6H_4CH_2CH{=}CH_2]\}\{\kappa^3\text{-}P,O,P\text{-}[xant(P^iPr_2)_2]\}$ (**8**) and $PhCH_2CH{=}CH(SiEt_3)$.

INTRODUCTION

Polyhydride complexes, L_nMH_x ($x \geq 3$), are transition metal species bearing enough hydrogen atoms bound to the metal center to form both classical hydride and dihydrogen ligands. A noticeable chemical characteristic of platinum group metal complexes of this class is their proven ability to promote σ-bond activation reactions.[1] Several features of the H-donor ligands explain the ability of such complexes to break σ-bonds. Classical hydrides behave as Brønsted bases facilitating the heterolytic split, whereas dihydrogen ligands display tendency to be released from the metal center generating highly unsaturated species that promote the homolytic cleavage. The activation produces an increase in the coordination number of the metal center of a coordinatively congested species and, in some cases, the oxidation number of an ion already highly oxidized. Consequently, activations involving E–H bonds are favored since the initial coordination number and oxidation of the metal center are rapidly restored after the activation, by removal of molecular hydrogen. Among the activated E–H bonds the C–H are predominant.[1,2] On the other hand, the Si–

H bond activation has received scarce attention,[3] although some silyl-metal-polyhydride derivatives are known mainly for osmium,[4] and iridium.[5] Like the metal-mediated C–H bond cleavage, the Si–H bond activation takes place via σ-intermediates, where the Si–H bond coordinates to the metal center. Nevertheless, a greater variety in the strength degrees has been described for the interactions M–HSi than for the M–HC ones.[6] The Si–H bond activation reactions are noticeable because of the relevance of the M–SiR_3 derivatives as intermediate species in the synthesis of chorosilanes,[7] the SiH/OH coupling,[8] and the hydrosilylation of unsaturated organic substrates,[9] including alkynes.[10]

Alkynes are fundamental molecules in organic synthesis,[11] which display great relevance in organometallics due to their use as precursors of different functional groups[12] and as building blocks in the formation of new ligands and interesting metallacycles.[13] Their reactions with transition metal hydride-complexes allow to generate single, double, and triple M–C bonds, depending on the nature of the metal center, the ligands, and the substituents of the alkyne.[12] Increasing the number of hydride ligands of the complex facilitates the use of alkyne building blocks, since it permits to enlarge the number of such molecules accessing into the metal center, as consequence of the increment of the number of possible reactions. The presence of higher number of organic fragments attached to the metal favors a higher variety of C–C coupling reactions.[14] Polyhydride complexes have the ability of activating the C(sp)–H bond of terminal alkynes, whereas they hydrogenate the C–C triple bond of the disubstituted ones. The activation usually leads to alkynyl species, which are able to act as efficient catalyst precursors in the dimerization of such substrates to afford both enynes and butatrienes;[15] skeletons of great interest because are present in some biologically active natural products and in synthetic intermediates for the preparation of highly substituted aromatic rings, and by their connection with material

science.[16] Terminal propargylic alcohols, HC≡CCR^{1}R^2(OH), are alcohol-functionalized alkynes widely employed in organic synthesis, as multifunctional reagents,[17] and in organometallics as allenylidene ligand precursors.[18] Although they are noticeable molecules by both reasons, their reactions with polyhydride complexes have not been studied.

Pincer ligands are having a dramatic impact in the modern coordination chemistry due to their ability to stabilize less common coordination polyhedra, which favor unusual oxidation states of the metal.[19] Polyhydride chemistry is not alien to this influence,[19a] although such ligands have been comparatively much less employed than in other areas, probably because pincer ligands saturate three coordination positions, reducing the number of sites for the hydrides. In this context, hemilabile pincer ligands are of great interest. A particular class with this characteristic is the *P,O,P*-diphosphines.[20] Among them, 9,9-dimethyl-4,5-bis(diisopropylphosphino)xanthene(xant(P^{i}Pr$_2$)$_2$) occupies a prominent place due of its coordinating flexibility.[21] Although the κ^3-*P,O,P-mer* mode is its most usual coordination,[8d;21c;22] complexes bearing the diphosphine κ^3-*P,O,P-fac*,[21c;23] κ^2-*P,P-cis*,[24] and κ^2-*P,P-trans*[21c;25] are also known. Transformations involving (xant(P^{i}Pr$_2$)$_2$)-M derivatives suggest that this ether-diphosphine changes its disposition at the metal coordination sphere to be adapted to the thermodynamic needs of the reactions. As a result, a wide variety of ruthenium,[22b,e] osmium,[22b,e,f,j;23a,b;24a,c] rhodium,[8d;21c;22a,c,d,g,h,k,l,n;24b,d] and iridium[8d;22a,b,i,m;24e] complexes stabilized by this diphosphine have been reported in the last years, which undergo fascinating transformations and promote interesting reactions, including catalytic processes.[8d;22b-d,h,k-m;24a,b,d,e;26] Accordingly, in 2013 we reported that sodium hydride in tetrahydrofuran removes the chloride ligands of OsCl$_2${κ^3-*P,O,P*-[xant(P^{i}Pr$_2$)$_2$]}{κ^1-*S*-[DMSO]} to give the hexahydride derivative OsH$_6${κ^3-*P,O,P*-[xant(P^{i}Pr$_2$)$_2$]}, under 3 atm of hydrogen, at 50 ºC. This κ^2-*P,P-trans*-

diphosphine-osmium(VI)-polyhydride slowly loses a hydrogen molecule, in methanol, under argon atmosphere, at temperatures higher than 293 K. The coordination of the oxygen atom to the metal center stabilizes the tetrahydride derivative $OsH_4\{\kappa^3\text{-}P,O,P\text{-}[xant(P^iPr_2)_2]\}$. In contrast to its precursor, this tetrahydride bears a κ^3-*P,O,P*-*mer*-diphosphine (Scheme 1).[24a]

Scheme 1. Synthesis of $OsH_4\{\kappa^3\text{-}P,O,P\text{-}[xant(P^iPr_2)_2]\}$

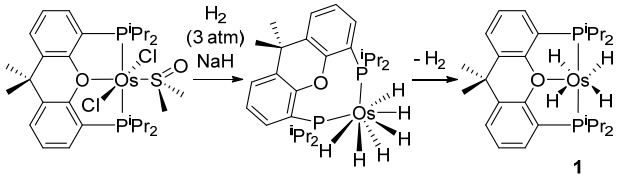

The handy availability of the tetrahydride complex along with the hemilability of the diphosphine, also proven in the hydrides chemistry as shown in Scheme 1, prompted us to investigate the tetrahydride-promoted Si–H bond activation of silanes. We searched for a silyl-osmium-polyhydride system allowing us to study the reactivity of such class of complexes with alkynes, including alkynols. This paper describes such activation, including its mechanism, and the reactions of the resulting pohyhydride species with 1,1-diphenyl-2-propyn-1-ol and 1-phenyl-1-propyne.

RESULTS AND DISCUSSION

Si–H Bond Activation of Tertiary Silanes. In spite of its saturated character, tetrahydride-osmium (IV) complex $OsH_4\{\kappa^3\text{-}P,O,P\text{-}[xant(P^iPr_2)_2]\}$ (**1**) activates the Si–H bond of triethylsilane, triphenylsilane, and 1,1,1,3,5,5,5-heptamethyltrisiloxane. Treatment of solutions of this polyhydride in toluene, with 2.0 equiv of the silane, under reflux, for 16 h leads to the corresponding derivatives $OsH_3(SiR_3)\{\kappa^3\text{-}P,O,P\text{-}[xant(P^iPr_2)_2]\}$ (SiR_3 = $SiEt_3$ (**2**), $SiPh_3$ (**3**),

$SiMe(OSiMe_3)_2$ (**4**)) and molecular hydrogen. These silyl-osmium(IV)-trihydride compounds were isolated as white solids in high yield 77-97%, in accordance with Scheme 2.

Scheme 2. Reaction of $OsH_4\{\kappa^3$-*P,O,P*-[xant($P^iPr_2)_2$]} with Tertiary Silanes

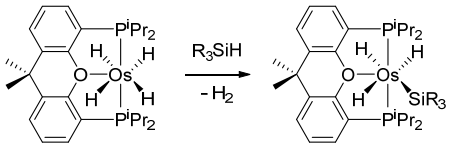

1

SiR_3 = $SiEt_3$ (**2**), $SiPh_3$ (**3**), $SiMe(OSiMe_3)_2$ (**4**)

The presence of a silyl ligand in complexes **2**-**4** is proved by the X-ray structure of the triphenylsilyl derivative **3**. Figure 1 shows the molecular diagram. The polyhedron around the metal center can be idealized as a pentagonal bipyramid. The ether-diphosphine, which is coordinated in the *mer*-fashion, disposes the P^iPr_2 arms at apical positions forming a P−Os−P angle of 158.63(4)º. The base is defined by the oxygen atom, the silyl group, and the hydride ligands. The oxygen atom is situated between H(01) and H(02), whereas the silyl group lies between H(01) and H(03). The classical-polyhydride nature of these compounds is supported by the separations between the hydrides H(02) and H(03) of 1.71(4) Å, obtained from the X-ray diffraction analysis, and 1.826 Å calculated for the DFT optimized structure. Both the X-ray structure and that DFT calculated reveal relatively short separations between the silicon atom and the hydrides H(01) and H(03) of 2.16(3) and 2.21(3) Å and 2.241 and 2.230 Å, respectively, which could suggest the existence of the denoted "*secondary interactions between silicon and hydrogen atoms* (SISHA)" (1.9-2.4 Å).[3,6b] Nevertheless, Atoms in Molecules (AIM) calculations do not show any bond path running between the involved atoms (Figure S1). Thus, such values seem to be a consequence of the size of the atoms and their positions in the complex, but not of the presence of any bonding interaction between them. In this context, we note that the boron-counterpart $OsH_2(\eta^2$-H-Bcat)$\{\kappa^3$-

P,O,P-[xant(P^iPr_2)$_2$]} (HBcat = catecholborane) is in contrast to **2**-**4** a hydride-osmium(II)-(σ-borane) derivative.[22f] Although there is a marked diagonal relationship between boron and silicon,[27] it seems that the stronger acidity of boron with regard to silicon favors the hydrogen-heteroatom interaction in this case.

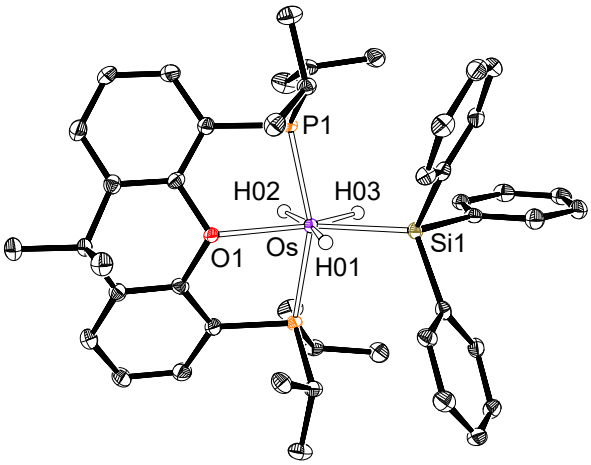

Figure 1. Molecular diagram of complex **3** (ellipsoids shown at 50% probability). All hydrogen atoms (except the hydrides) are omitted for clarity. Selected bond distances (Å) and angles (deg): Os–P(1) = 2.3061(6), Os–O(1) = 2.284(2), Os–Si(1) = 2.3862(9); P(1)–Os–P(1) = 158.63(4), O(1)–Os–Si(1) = 145.97(6).

Hydrides H(02) and H(03) undergo a thermally activated site exchange process in toluene-d_8, which occurs with low activation energy (Table 1). Thus, at 313 K, the high field region of the ^{1}H NMR spectra of the three polyhydrides shows two resonances, in a 1:2 intensity ratio, at about –1 ppm and between –10.0 and –12.5ppm. The first of them due to H(01) and the second one corresponding to H(02) and H(03). Between 283 and 223 K, depending on the silyl ligand, decoalescence of the higher field signal takes place to afford two resonances. Accordingly, at temperatures lower than 223 K, the spectra display a resonance for each inequivalent hydride ligand, at the chemical shifts collected in Table 1. The 300 MHz $T_{1(min)}$ values for the resonance

assigned to the hydride ligands H(02) and H(03) of **2** and **3** were also determined at 248 and 230 K, respectively. The obtained values of 231±3 (**2**) and 251±3 (**5**) ms lead to separations between such hydrides of 1.76 (**2**) and 1.79 (**3**) Å,[28] which compare very nicely with those obtained from the X-ray diffraction analysis and DFT calculations for **3**. In agreement with the structure shown in Figure 1, the $^{31}P\{^{1}H\}$ NMR spectra of **2**-**4** show a singlet between 54 and 47 ppm, as expected for the equivalent $P^{i}Pr_2$ arms of the diphosphine. A characteristic feature for these compounds is also the presence of a triplet ($^{2}J_{Si-P} \approx 5$ Hz) at about 2 ppm for a **2** and **3** and at –19.8 ppm for **4**, in the respective $^{29}Si\{^{1}H\}$ NMR spectrum.

Table 1. Coalescence Temperature (T_c), Activation Energy ($\Delta G^{\ddagger}$) for Site Exchange Process and NMR Chemical Shift for the Hydride Ligands of Complexes 2-4.

Complex	T_c (K)	$\Delta G^{\ddagger}$ (kcal·mol^{-1})	Chemical Shift (ppm)		
2	278	10.9 ± 0.2	–1.76	–4.01	–20.21
3	248	9.8 ± 0.2	–0.14	–3.73	–17.08
4	228	8.9 ± 0.2	–1.53	–4.42	–18.85

Mechanism of the Si–H Bond Activation. Complex **1** is a coordinately saturated species. Thus, the Si–H bond activation of the silanes requires the previous generation of a coordination vacancy at the metal center. In principle, such process could occur in two different manners (Scheme 3): by reductive elimination of molecular hydrogen (route *a*) and through the dissociation of the hemilabile ether function of the diphosphine (route *b*). In the first case, the activation would take place via osmium(II) intermediates; the unsaturated dihydride $\mathbf{a_1}$ should coordinate the Si–H bond of the silanes to afford the osmium(II) σ-intermediates $\mathbf{a_2}$, which could evolve into **2**-**4** by homolytic rupture of the coordinate σ-bond. In the second one, the activation involves

intermediates of osmium(IV) and osmium(VI); similarly, to $\mathbf{a_1}$, the unsaturated osmium(IV)-tetrahydride $\mathbf{b_1}$ should coordinate the Si–H bond of the silanes to give the osmium(IV) σ-intermediates $\mathbf{b_2}$. These intermediates could lead to **2-4** by means of two different pathways associated to the type of activation undergone by the coordinated σ-bond. A hydride-promoted heterolytic rupture should directly give the silyl-osmium(IV)-trihydride derivatives, whereas a homolytic activation followed by reductive elimination of molecular hydrogen would afford the silyl products via silyl-osmium(VI)-pentahydride intermediates $\mathbf{b_3}$. Complexes with two triisopropylphosphine ligands instead of an ether-diphosphine resembling to $\mathbf{b_3}$ have been recently isolated and fully characterized, including the X-ray analysis structure of one of them, in our laboratory.[29]

Scheme 3. Proposed Reaction Pathway for the $OsH_3(SiR_3)\{\kappa^3$-*P,O,P*-[xant(P^iPr_2)$_2$]} Formation

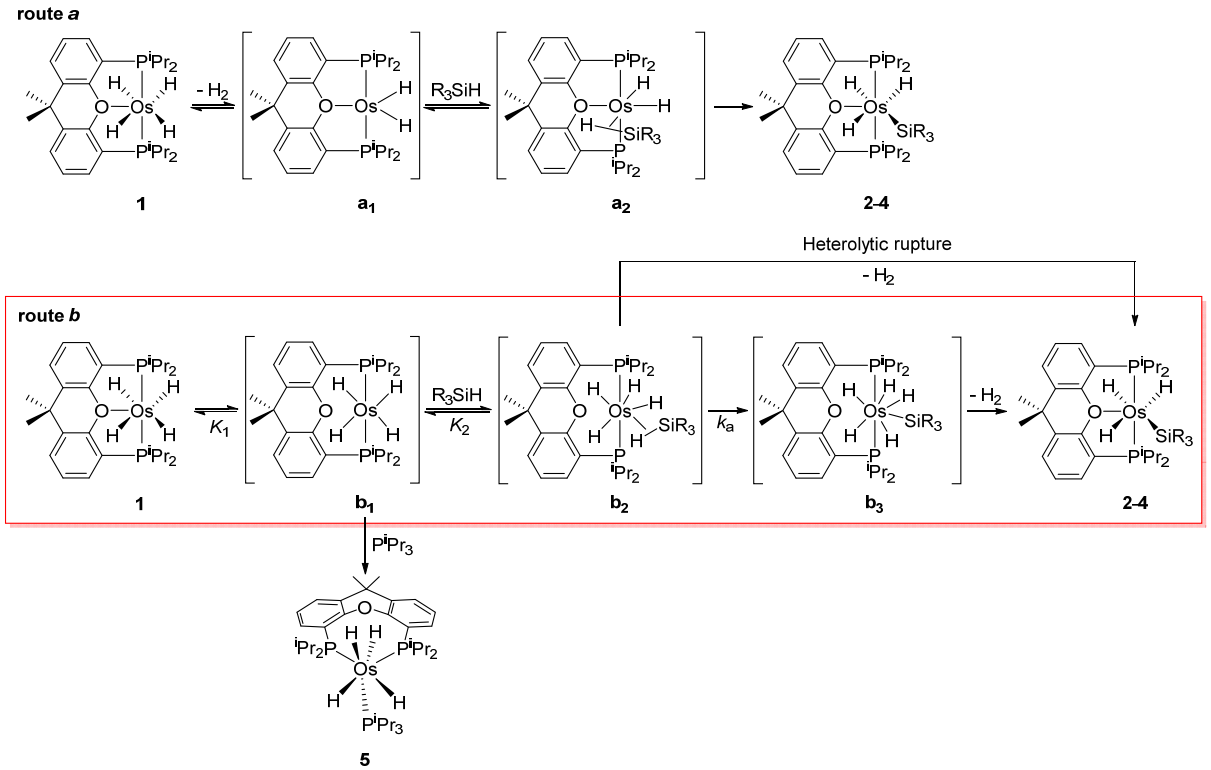

We reasoned that the use of R_3SiD instead of R_3SiH should allow to discern between routes *a* and *b* and to establish the nature of the Si–H rupture. Indeed, route *a* should afford one deuterium atom at the hydride position, whereas a hydride-promoted heterolytic rupture through route *b* should lead to a totally protiated product. On the other hand, the homololytic activation to form intermediate **b3** would permit a deuterium amount intermediate between cero and one at the metal center, since the position exchange processes, typical in this class of pentahydride complexes, should carry to the deuterium atom to different positions, before the reductive elimination. Addition of 2.0 equiv of $(Me_3SiO)_2MeSiD$ to a solution of **1**, in toluene-d_8, at 110 ºC leads to a partially deuterated **2-$d_{0.5}$** species containing 0.5 deuterium atoms distributed between the H(02) and H(03) positions (Figure S49). As above mentioned, such deuterium amount at the metal center supports the route *b* through intermediate **b3**, as the preferred one for the Si–H bond activation promoted by **1**.

To gain an additional evidence in favor of the route *b*, we decided to trap the intermediate **b1** with a 2e- donor ligand such as triisopropylphosphine. In methanol, the stirring of **1** in presence of 1.0 equiv of the phosphine affords the expected tetrahydride $OsH_4\{\kappa^2\text{-}P,P\text{-}[xant(P^iPr_2)_2]\}(P^iPr_3)$ (**5** in Scheme 3), which was isolated as a white solid in 78% yield and characterized by X-ray diffraction analysis. Figure 2 gives a view of the structure. The disposition of donor atoms around the metal center can be described as a piano stool geometry of ideal C_s symmetry, where the four-membered face is formed by the phosphorous atoms of the chelating diphosphine and the hydrides H(01) and H(04), whereas the three-member face is defined by the hydrides H(02) and H(03) and the phosphorus atom of the triisopropylphosphine. Such ligand disposition is unusual for osmium(IV)-tetrahydride complexes of the class $OsH_4(PR_3)_3$, which generally display a pentagonal bipyramid arrangement.[30] In solution in toluene-d_8, the structure is not rigid in

accordance with the similar stability of the usual four geometries of seven-coordinate complexes and the low activation energy for their interconversion.[31] Thus, the ^{1}H NMR spectrum at room temperature shows a broad resonance for the four hydride ligands at –10.87 ppm, which splits into two broad signals, at –9.99 and –11.90 ppm, of 1:1 intensity ratio, at 235 K. The $^{31}P\{^{1}H\}$ spectrum is also temperature dependent (Figure S27). At room temperature, the spectrum shows at 44.6 ppm an apparent triplet due to the monodentate phosphine and at 8.4 ppm a broad signal corresponding to the diphosphine. At temperatures lower than 253 K, the triplet is transformed in a complex signal, whereas the broad resonance splits into two signals at 14.7 and 2.3 ppm.

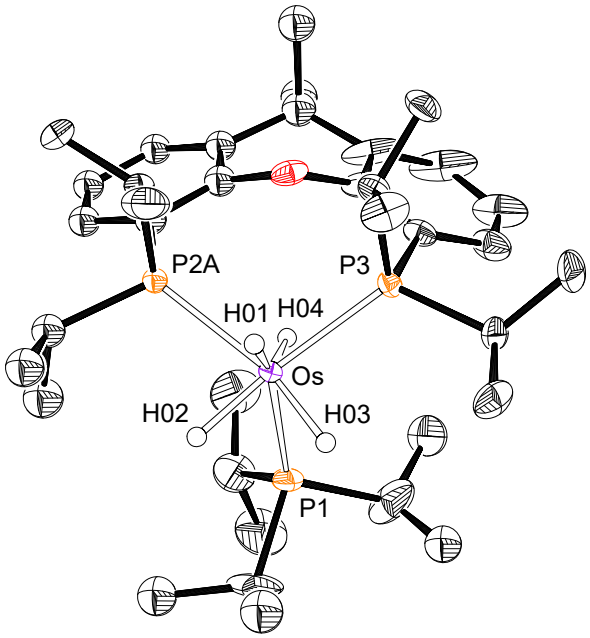

Figure 2. Molecular diagram of complex **5** (ellipsoids shown at 50% probability). All hydrogen atoms (except the hydrides) are omitted for clarity. Selected bond distances (Å) and angles (deg): Os–P(1) = 2.3128(9), Os–P(2A) = 2.3433(11), Os–P(3) = 2.3540(7); P(2A)–Os–P(3) = 105.43(4), P(1)–Os–P(3) = 115.40(3).

Once established the pathway for the Si–H bond activation, we decided to confirm it and to ascertain the rate determining step by means the kinetics investigation of the reaction of **1** with Et_3SiH. The transformation of **1** into **2**, studied by $^{31}P\{^1H\}$ NMR spectroscopy, was performed under *pseudo*-first order conditions, at 353 K, for concentrations of silane ([Et_3SiH]) between 0.38 and 0.76 M, and starting from a concentration of **1** of 1.9×10^{-2} M ($[\mathbf{1}]_0$). In this range of silane concentrations, the consumption of **1** with the corresponding increase of the amount of **2** is an exponential function of time, which can be linearized (Figure 3) according to the expression shown in eq 1, where [**1**] is the concentration of tetrahydride at the time *t*. Table 2 collects the rate constants k^{obs} for each silane concentration.

$$ln\frac{[\mathbf{1}]}{[\mathbf{1}]_0} = -k^{obs}t \qquad (1)$$

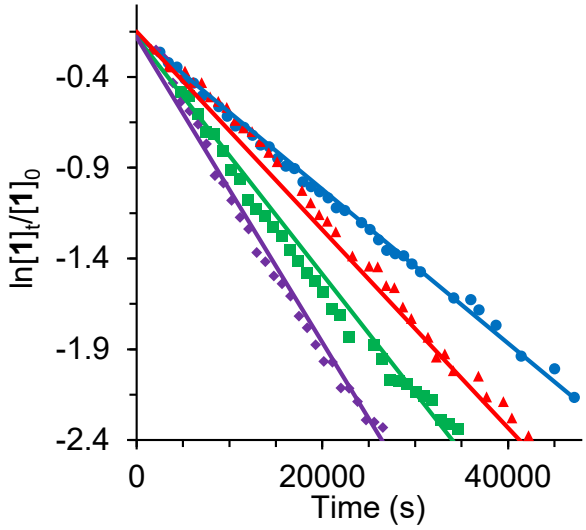

Figure 3. Plot of eq 1 for reaction of **1** (1.9×10^{-2} M) with different concentrations of triethylsilane in toluene-d_8. [Et_3SiH] = 0.38 M (blue ●); 0.48 M (red ▲); 0.57 M (green ■); 0.76 M (purple ♦).

Table 2. Kinetic data of the reaction of 1 with Et_3SiH in toluene-d_8.

T (K)	[Et_3SiH] (M)	k^{obs} ($\times 10^5$ s^{-1})	k ($\times 10^4$ M^{-1} s^{-1})
353	0.38	4.24 ± 0.10	1.11 ± 0.10
353	0.48	5.46 ± 0.11	1.15 ± 0.11
353	0.57	6.53 ± 0.19	1.15 ± 0.19
353	0.76	8.41 ± 0.24	1.10 ± 0.24

Constant k^{obs} is a function of [Et_3SiH] according to eq 2. A plot of lnk^{obs} versus ln[Et_3SiH] yields a straight line of slope 0.98 (Figure S54), revealing that the activation is also first order in silane concentration (*a* = 1 in eq 2) and therefore the rate law is that given in eq 3. A plot of k^{obs} versus [Et_3SiH] (Figure 4) provides a value for *k* of (1.1 ± 0.1) × 10^{-4} M^{-1} s^{-1}.

$$k^{obs} = k[Et_3SiH]^a \quad (2)$$

$$-\frac{d[\mathbf{1}]}{dt} = k[\mathbf{1}][Et_3SiH] \quad (3)$$

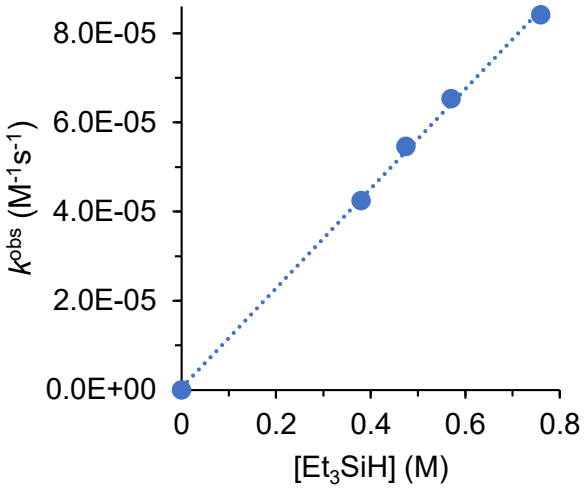

Figure 4. Plot of k^{obs} versus [Et_3SiH] for the reaction of **1** (0.019 M) with Et_3SiH in toluene-d_8 at 353 K.

The rate of the reaction of **1** with Et_3SiD is significantly slower than that with Et_3SiH. The ratio k_H/k_D gives a primary isotope effect of 4.2, which strongly supports the homolytic cleavage of the Si–H bond as the rate-determining step in the formation of the silyl-osmium(IV)-trihydride complexes.[32] According to the rate-determining step approximation, the formation of **2** can be also described by eq 4.

$$-\frac{d[\mathbf{1}]}{dt} = k_a[\boldsymbol{b_2}] \qquad (4)$$

Since the reductive elimination of molecular hydrogen from intermediate $\mathbf{b_3}$ is the fast step of the silyl product formation, the concentration of the intermediate $\mathbf{b_2}$ can be calculated as follows:

$$[\mathbf{1}] = [\mathbf{1}]_{eq} + [\boldsymbol{b_1}] + [\boldsymbol{b_2}] \qquad (5)$$

Because $[\mathbf{1}]_{eq} = [\mathbf{b_2}] / K_1K_2[Et_3SiH]$ and $[\mathbf{b_1}] = [\mathbf{b_2}] / K_2[Et_3SiH]$, we have:

$$[\boldsymbol{b_2}] = \frac{K_1K_2[\mathbf{1}][Et_3SiH]}{1 + K_1 + K_1K_2[Et_3SiH]} \qquad (6)$$

Intermediate $\mathbf{b_1}$ is not spectroscopically detected. As a consequence, we can assume that $K_1 + K_1 K_2[Et_3SiH] \ll 1$, and therefore $[\mathbf{b_2}]$ can be described as follows:

$$[\boldsymbol{b_2}] = K_1K_2[\mathbf{1}][Et_3SiH] \qquad (7)$$

Combining eqs 4 and 7, we obtain eq 8, which is an additional evidence in favor of route *b* and reveals that $k = k_aK_1K_2$; i.e., the experimental rate constant k is proportional to the rate constant k_a and the equilibrium constants K_1 and K_2.

$$-\frac{d[\mathbf{1}]}{dt} = k_aK_1K_2[\mathbf{1}][Et_3SiH] \qquad (8)$$

Reactions with Alkynes. Treatment of solutions of **2** in toluene with 4.0 equiv of 1,1-diphenyl-2-propyn-1-ol, at 80 ºC, for 2 h leads to the hydroxyvinylidene-osmium(II)-(bishydroxyalkynyl)

derivative Os{C≡CC(OH)Ph$_2$}$_2${=C=CHC(OH)Ph$_2$}{κ^3-*P,O,P*-[xant(P^{i}Pr$_2$)$_2$]} (**6**), which was isolated as a brown solid in 52% yield. In methanol, the hydroxyvinylidene ligand dehydrates. Thus, the stirring of suspensions of **6** in the alcohol, for 4 h, at room temperature affords the allenylidene complex Os{C≡CC(OH)Ph$_2$}$_2${=C=C=CPh$_2$}{κ^3-*P,O,P*-[xant(P^{i}Pr$_2$)$_2$]} (**7**), which was obtained as a green solid in 85% yield (Scheme 4).

Scheme 4. Reaction of OsH$_3$(SiEt$_3$){κ^3-*P,O,P*-[xant(P^{i}Pr$_2$)$_2$]} with 1,1-Diphenyl-2-propyn-1-ol

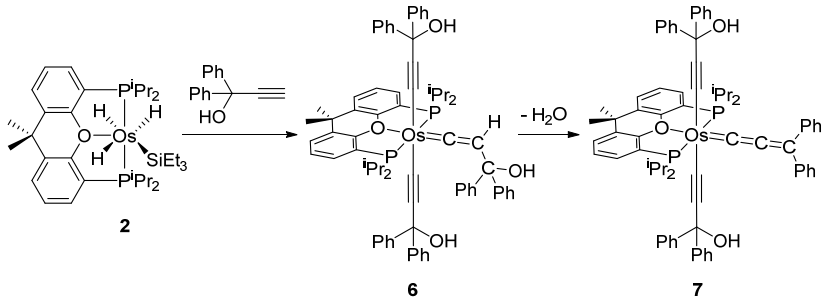

Complex **6** was characterized by X-ray diffraction analysis. Figure 5 shows a view of the structure. With the ether-diphosphine *mer*-disposed (P(1)–Os–P(2) = 162.36(3)º), the coordination polyhedron defined by the donor atoms around the metal center is the expected octahedron for a six-coordinate d^6-species. The hydroxyalkynyl ligands are mutually *trans*-situated, forming an angle C(16)–Os–C(31) of 168.57(12)º, whereas the π-acceptor hydroxyvinylidene group lies *trans* to the π-donor oxygen atom of the pincer (C(1)–Os–O(4) = 176.13(10)º). The metal-alkynyl bond lengths Os–C(16) and Os–C(31) of 2.068(3) Å are consistent with an Os–C(sp) single bond[33] and suggest a low degree of osmium-to-ligand back-bonding.[34] As in other osmium-vinylidene compounds,[35] the vinylidene ligand binds to the osmium atom in a nearly linear fashion stablishing an angle Os–C(1)–C(2) of 175.2(3)º. Distances Os–C(1) and C(1)–C(2) of 1.820(3) and 1.316(4)

Å, respectively, also compare well with those previously reported for complexes of this class and strongly support the presence of double bonds between the involved atoms. In benzene-d_6, at room temperature, the vinylidene ligand rotates around the metal-vinylidene axis, as is usual for this class of compounds. Thus, the $^{13}C\{^1H\}$ NMR spectrum reveals the presence of only one type of hydroxyalkynyl ligands; the atoms C_α and C_β of the triple bond give rise to a triplet ($^2J_{C-P}$ = 11.8 Hz) at 102.0 ppm and a singlet at 75.5 ppm, respectively, while the C_α and C_β atoms of the vinylidene ligand generate two triplets, at 291.6 ($^2J_{C-P}$ = 9.1 Hz) and 111.5 ($^3J_{C-P}$ = 3.8 Hz) ppm, respectively. In the ^1H NMR spectrum, the most noticeable resonance is that due to the $C_\beta H$-hydrogen atom of the vinylidene moiety, which appears at 2.45 ppm as a triplet ($^4J_{H-P}$ = 2.7 Hz). The $^{31}P\{^1H\}$ NMR spectrum displays a singlet at 12.7 ppm, as expected for equivalent P^iPr_2 arms.

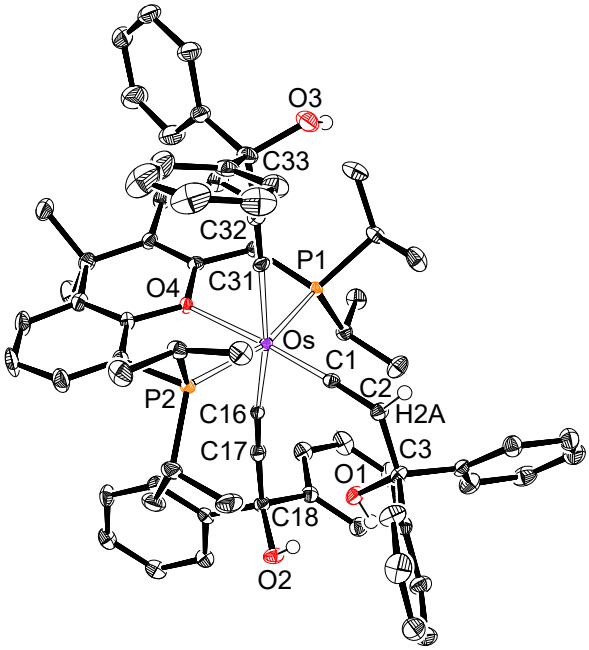

Figure 5. Molecular diagram of complex **6** (ellipsoids shown at 50% probability). All hydrogen atoms (except the C_β–H and OH) are omitted for clarity. Selected bond distances (Å) and angles

(deg): Os–P(1) = 2.3489(7), Os–P(2) = 2.3373(7), Os–O(4) = 2.262(2), Os–C(16) = 2.068(3), Os–C(31) = 2.068(3), Os–C(1) = 1.820(3), C(1)–C(2) = 1.316(4); P(1)–Os–P(2) = 162.36(3), C(1)–Os–O(4) = 176.13(10), C(16)–Os–C(31) = 168.57(12).

Complex **7** was also characterized by X-ray diffraction analysis. Figure 6 gives a molecular diagram of the species. The geometry around the metal center resembles that of **6**, with the allenylidene group in the position of the hydroxyvinylidene ligand. The C_3-cumulene binds to the osmium atom in a nearly linear fashion (Os−C(1)−C(2) = 178.7(3)° and C(1)−C(2)−C(3) = 174.0(4)°). Distances throughout the metal-cumulene chain of 1.868(4) Å (Os–C(1)), 1.265(5) Å (C(1)–C(2)), and 1.311(5) Å (C(2)–C(3)) compare well with those previously reported for structurally characterized complexes of this class. In agreement with them, the C(1)−C(2) and C(2)−C(3) values suggest a notable contribution of the canonical form $[M]^{-}-C\equiv C-C^{+}Ph_2$ to the structure of the cumulene.[22b,23b,36] The C_3-chain gives rise to three triplets, in the $^{13}C\{^1H\}$ NMR spectrum, which in benzene-d_6 appear at 251.3 (C_α, $^2J_{C-P}$ = 10.1 Hz), 247.3 (C_β, $^3J_{C-P}$ = 3.7 Hz), and 154.2 (C_γ, $^4J_{C-P}$ = 2.1 Hz) ppm. Noticeable resonances of this spectrum are also a triplet ($^2J_{C-P}$ = 11.7 Hz) at 103.8 ppm and a singlet at 75.1 ppm, respectively, corresponding to the C_α and C_β atoms of the triple bond of the hydroxyalkynyl ligands. In agreement with **6**, the $^{31}P\{^1H\}$ spectrum displays a singlet at 13.3 ppm.

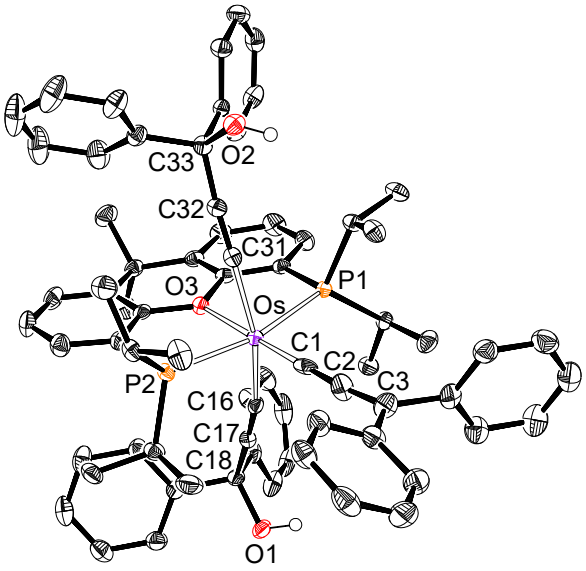

Figure 6. Molecular diagram of complex **7** (ellipsoids shown at 50% probability). All hydrogen atoms (except OH) are omitted for clarity. Selected bond distances (Å) and angles (deg): Os–P(1) = 2.3254(8), Os–P(2) = 2.3337(8), Os–O(3) = 2.246(2), Os–C(16) = 2.067(3), Os–C(31) = 2.067(3), Os–C(1) = 1.868(4), C(1)–C(2) = 1.265(5), C(2)–C(3) = 1.311(5); P(1)–Os–P(2) = 163.46(3), C(1)–Os–O(3) = 177.63(11), C(16)–Os–C(31) = 157.89(12), Os–C(1)–C(2) = 178.7(3), C(1)–C(2)–C(3) = 174.0(4).

Complex **6** is a triol-functionalized counterpart of complexes $Os(C{\equiv}CR)_2(=C=CHR)\{xant(P^iPr_2)_2\}$ (R = Ph, ^{t}Bu). Such vinylidene-osmium(II)-bis(alkynyl) derivatives efficiently catalyze the stereoselective head-to-head (*Z*)-dimerization of terminal alkynes to afford the corresponding enynes (*Z*)-RC≡CCH=CHR.[24a] In accordance with this, complex **2** promotes the head-to-head (*Z*)-dimerization of 1,1-diphenyl-2-propyn-1-ol via the active species **6**, which is generated *in situ*. The reactions were performed in a closed system, at 110 ºC and 140 ºC, in toluene, using a 5 mol% of osmium precursor. At 110 ºC, the dimerization

selectively affords (*Z*)-1,1,6,6-tetraphenylhex-2-en-4-yne-1,6-diol in 70% yield after 2 h. At 140 ºC, the hydroxy group at 1-position of the enyne adds to the C–C triple bond to produce the furanol derivative (*E*)-2-(5,5-diphenylfuran-2(*5H*)-ylidene)-1,1-diphenylethan-1-ol in 80% yield after 24 h (Scheme 5).

Scheme 5. Head-to-head (*Z*)-Dimerization of 1,1-Diphenyl-2-propyn-1-ol and Formation of the Furanol Derivative

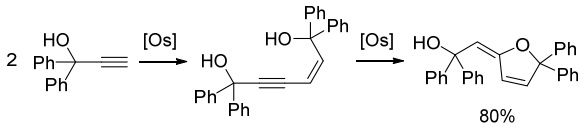

Scheme 5 summarizes a rare example of tandem catalyzed reaction,[37] which has not any precedent in the osmium chemistry. The process involves the dimerization of the functionalized alkyne and the subsequent cycloisomerization of the resulting enynediol to afford an interesting furanylideneethanol. The formation of the five-membered heterocycle is noteworthy, since such moiety is present as structural subunit in numerous natural products with a variety of applications in several fields. Metal catalysts for the dimerization of terminal propargylic alcohols are scarce. In contrast to **6**, the majority of them leads to products resulting from a head-to-head (*E*)-coupling[38] and in some case from a head-to-tail dimerization.[39] The formation of alkylidenebenzocyclobutenyl alcohols has been also observed.[40] Catalysts for the cycloisomerization of enynols are even more rare[41] and, as far as we know, have not applied to diols.

Complex **2** also reacts with internal alkynes such as 1-phenyl-1-propyne. Treatment of its solutions in toluene with 2.0 equiv of the hydrocarbon, under reflux, for 16 h leads to OsH{κ^1-

C,η^2-[$C_6H_4CH_2CH{=}CH_2$]}{κ^3-*P,O,P*-[xant(P^iPr_2)$_2$]} (**8**) and (*E*)-triethyl(3-phenylprop-1-en-1-yl)silane. The reaction can be rationalized according to Scheme 6. Complex **2** could initially reduce 1.0 equiv of the internal alkyne to afford the unsaturated silyl-osmium(II)-hydride intermediate $\mathbf{c_1}$ and 1-pheny-1-propene. Under the reaction conditions the generated olefin should isomerize from internal to terminal. Thus, the silyl-osmium(II)-hydride species $\mathbf{c_1}$ could promote the dehydogenative silylation of the resulting 3-phenyl-1-propene, in the presence of a second equiv of internal alkyne that should act as hydrogen acceptor. As a result, the silylated olefin at the terminal position, an osmium(0) intermediate $\mathbf{c_2}$, and 1-phenyl-1-propene again would be formed. The isomerization of 1-phenyl-1-propene to 3-phenyl-1-propene, followed by the C–C double bond assisted activation of an *ortho*-CH bond of the phenyl substituent of the latter, promoted by intermediate $\mathbf{c_2}$, should finally afford the organometallic product**.**

Scheme 6. Reaction of $OsH_3(SiEt_3)$}{κ^3-*P,O,P*-[xant(P^iPr_2)$_2$]} with 1-Phenyl-1-propyne

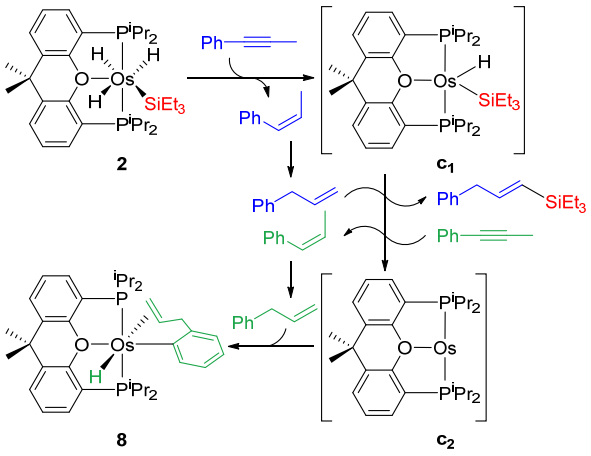

Complex **8** was obtained as a yellow solid in 65% yield and characterized by X-ray diffraction analysis. Figure 7 shows a view of the molecule. The coordination around the osmium atom can

be described as a very distorted octahedron. The distortion is consequence of the steric hindrance experienced by the P^iPr_2 arms of the *mer*-disposed ether-diphosphine and the olefinic C(8)–C(9) bond and explains why only one from the two olefins generated in the reaction selectively attaches to the osmium atom; the olefin with less steric hindrance in its C–C double bond. The parallel disposition of the olefinic C(8)–C(9) bond to the P(1)–Os–P(2) axis decreases the phosphine bite angle until 141.44(6)º, a value strongly deviated from the ideal of 180º. In agreement with the concerted character of the oxidative addition of the C–H bond, the hydride ligand H(01) and the metalated carbon atom C(1) of the phenyl group are mutually *cis* disposed. The oxygen atom of the diphosphine lies *trans* to the phenyl group (O(1)–Os–C(1) = 168.0(2)º), whereas the C(8)–C(9) bond situates *trans* to H(01). The C(8)–C(9) bond coordinates to the osmium atom with Os–C(8) and Os–C(9) distances of 2.173(6) and 2.178(6) Å, which are almost identical. The coordination causes a significant elongation of the double bond, as expected for the Chatt−Dewar−Ducanson bonding model. Thus, the C(8)–C(9) bond length of 1.424(9) Å is notably longer than those usually observed for free C–C double bonds of around 1.34 Å.[42] In accordance with a strong addition of this bond to the metal center, the resonances corresponding to C(8) and C(9) are observed at significant high field, 41.0 and 36.3 ppm, respectively, in the $^{13}C\{^1H\}$ NMR spectrum in benzene-d_6. In a consistent manner, the signals due to the associated hydrogen atoms appear at 3.67 (C(8)H) and 2.49 and 1.84 ($C(9)H_2$) ppm in the ^1H NMR spectrum, which displays the hydride resonance at –7.15 ppm as a doublet of doublets with H–P coupling constants of 33.0 and 37.4 Hz. As a result of the asymmetry imposed by the coordination of the olefin, the P^iPr_2 arms of the pincer are inequivalent. Accordingly, the $^{31}P\{^1H\}$ NMR spectrum shows an AB spin system centered at 36.2 ppm and defined by $\Delta\nu$ = 726 Hz and $J_{A–B}$ = 164 Hz.

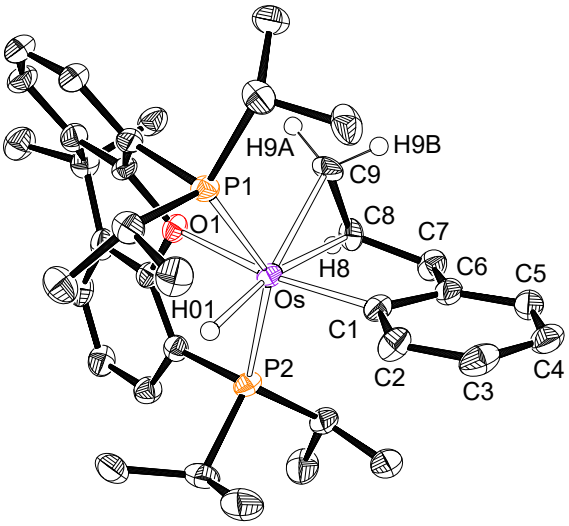

Figure 7. Molecular diagram of complex **8** (ellipsoids shown at 50% probability). All hydrogen atoms are omitted (except the hydride and the olefinic hydrogen atoms) for clarity. Selected bond distances (Å) and angles (deg): Os–P(1) = 2.2926(15), Os–P(2) = 2.2981(16), Os–O(1) = 2.254(4), Os–C(1) = 2.055(6), Os–C(8) = 2.173(6), Os–C(9) = 2.178(6); P(1)–Os–P(2) = 141.44(6), O(1)–Os–C(1) = 168.0(2).

CONCLUDING REMARKS

This study has revealed that the tetrahydride $OsH_4\{\kappa^3\text{-}P,O,P\text{-}[xant(P^iPr_2)_2]\}$ activates the Si–H bond of tertiary silanes to form silyl-osmium(IV)-trihydride derivatives, in spite of its saturated character. A detailed study of the mechanism of the activation pointed out that the activation is possible because of the hemilabile nature of the ether-diphosphine, which dissociates its oxygen atom to permit the Si–H coordination of the silane. The subsequent oxidative addition of the coordinated bond, followed by the reductive elimination of molecular hydrogen, affords the silylated polyhydrides. Kinetics of the addition and the observed primary isotope effect demonstrate that the rupture of the Si–H bond is the rate determining step of the metal silylation.

These silyl-osmium(IV)-trihydride complexes promote a catalytic tandem process, which converts 1,1-diphenyl-2-propyn-1-ol into an interesting furanylideneethanol, via the (*Z*)-enynediol intermediate. The catalysis takes place through the hydroxyvinylidene-osmium(II)-bis(hydroxyalkynyl) derivative $Os\{C{\equiv}CC(OH)Ph_2\}_2\{{=}C{=}CHC(OH)Ph_2\}\{\kappa^3\text{-}P,O,P\text{-}[xant(P^iPr_2)_2]\}$, which has been isolated and fully characterized. The dehydration of the hydroxyvinylidene group of this species yields an allenylidene derivative, which exemplified a novel class of organometallic compound in the osmium chemistry.

In summary the Si–H bond activation of silanes promoted by an osmium-tetrahydride, stabilized by a pincer ether-diphosphine, affords silyl-osmium(IV)-trihydride derivatives, which display an interesting reactivity towards alkynes, including the catalytic transformation of 1,1-diphenyl-2-propyn-1-ol into (*E*)-2-(5,5-diphenylfuran-2(*5H*)-ylidene)-1,1-diphenylethan-1-ol.

EXPERIMENTAL SECTION

General Information. All reactions were performed with rigorous exclusion of air and moisture at an argon/vacuum manifold using standard Schlenk-tube or glovebox techniques. Alkynes and silanes were purchased from commercial sources and distilled in a Kugelrohr distillation oven prior to use. Complex **1** was prepared according to the published method.[24a] Instrumental methods, X-ray and theoretical calculations details, NMR and IR spectra (Figures S2-S48) and kinetic and deuteration experiments (Figures S49-S54) are given in the Supporting Information. Coupling constants *J* and *N* ($N = J_{P–H} + J_{P'–H}$ for ^1H and $N = J_{P–C} + J_{P'–C}$ for $^{13}C\{^1H\}$) are given in hertz.

Preparation of $OsH_3(SiEt_3)\{\kappa^3\text{-}P,O,P\text{-}[xant(P^iPr_2)_2]\}$ (2). A solution of **1** (200 mg, 0.31 mmol) in toluene (5 mL) was treated with Et_3SiH (100 μL, 0.62 mmol). The resulting mixture was heated at reflux for 16 h. After that time, the mixture was concentrated to dryness to afford a yellowish

residue. Addition of methanol (5 mL) caused the precipitation of a white solid, which was washed with additional methanol (3 x 5 mL) and dried in vacuo. Yield: 182 mg (77%). Anal. Calcd for $C_{33}H_{58}OOsP_2Si$: C, 52.77; H, 7.78. Found: C, 52.48; H, 7.76. HRMS (*electrospray, m/z*) calcd. for $C_{27}H_{43}OOsP_2$ $[M - SiEt_3]^+$: 637.2416, found: 637.2398. IR (cm^{-1}) ν(Os–H) 1841 (m). ^1H NMR (400.13 MHz, toluene-d_8, 298 K) δ 7.14 (m, 2H, CH-arom, POP), 6.85 (m, 2H, CH-arom, POP), 6.82 (m, 2H, CH-arom, POP), 2.47 (m, 2H, PC*H*$(CH_3)_2$), 2.34 (m, 2H, PC*H*$(CH_3)_2$), 1.34 (t, $^3J_{H-H}$ = 10.4, 9H, Si$(CH_2CH_3)_3$), 1.31 (s, 3H, C(C*H*$_3)_2$), 1.27 (dvt, $^3J_{H-H}$ = 7.3, *N* = 16.9, 6H, PCH(C*H*$_3)_2$), 1.08 (dvt, $^3J_{H-H}$ = 5.6, *N* = 11.8, 6H, PCH(C*H*$_3)_2$), 1.05-0.97 (m, 18H, Si(C*H*$_2$CH$_3)_3$ + PCH(C*H*$_3)_2$), 0.93 (s, 3H, C(C*H*$_3)_2$), –1.72 (tt, $^2J_{H-H}$ = 3.3, $^2J_{H-P}$ = 9.6, 1H, OsH), –12.26 (vbr, 2H, OsH). ^1H NMR (400.13 MHz, toluene-d_8, 223 K, high-field region) δ –1.76 (m, 1H, OsH), –4.01 (m, 1H, OsH), –20.21 (m, 1H, OsH). $^{13}C\{^1H\}$-APT NMR (100.62 MHz, toluene-d_8, 298 K) δ 161.7 (vt, *N* = 13.0, C-arom, POP), 133.7 (vt, *N* = 4.9, C-arom, POP), 129.1 (s, CH-arom, POP), 129.0 (s, CH-arom, POP), 127.2 (vt, *N* = 27.0, C-arom, POP), 124.8 (s, CH-arom, POP), 34.7 (s, *C*$(CH_3)_2$), 32.1 (s, C(*C*$H_3)_2$), 27.8 (vt, *N* = 19.9, P*C*H$(CH_3)_2$), 23.8 (vt, *N* = 32.7, P*C*H$(CH_3)_2$), 22.1 (s, C(*C*$H_3)_2$), 21.0 (s, PCH(*C*$H_3)_2$), 19.2 (vt, *N* = 9.8, PCH(*C*$H_3)_2$), 19.0 (vt, *N* = 3.8, PCH(*C*$H_3)_2$), 15.8 (vt, *N* = 4.3, PCH(*C*$H_3)_2$), 14.9 (s, Si(*C*$H_2CH_3)_3$), 9.7 (s, Si(CH_2*C*$H_3)_3$). $^{31}P\{^1H\}$ NMR (161.98 MHz, toluene-d_8, 298 K) δ 50.0 (s). $^{29}Si\{^1H\}$ NMR (59.63 MHz, C_6D_6, 298 K) δ 2.0 (t, $^2J_{Si-P}$ = 4.6). $T_{1(min)}$ (ms, OsH, 300.13 MHz, toluene-d_8, 248 K) 231 ± 3 (−20.21 ppm).

Preparation of $OsH_3(SiPh_3)\{\kappa^3$-*P,O,P*-[xant($P^iPr_2)_2$]} (3). A solution of **1** (200 mg, 0.31 mmol) in toluene (5 mL) was treated with $HSiPh_3$ (164 mg, 0.62 mmol). The resulting mixture was heated at reflux for 16 h. After that time, the mixture was concentrated to dryness to afford a yellowish residue. Addition of methanol (5 mL) caused the precipitation of a white solid, which was washed with additional methanol (3 x 5 mL) and dried in vacuo. Yield: 275 mg (97%).

Colorless single crystals suitable for X-ray diffraction analysis were obtained from a saturated solution of **3** in benzene at room temperature. Anal. Calcd for $C_{45}H_{58}OOsP_2Si$: C, 60.38; H, 6.53. Found: C, 60.77; H, 6.51. HRMS (*electrospray, m/z*) calcd. for $C_{27}H_{43}OOsP_2$ $[M - SiPh_3]^+$: 637.2398, found 637.2371. IR (cm^{-1}) ν(Os–H) 1789 (m). ^1H NMR (400.13 MHz, toluene-d_8, 298 K) δ 8.15 (d, $^3J_{H–H}$ = 7.4, 6H, *o*-Ph), 7.23 (dd, $^3J_{H–H}$ = 7.4, $^3J_{H–H}$ = 7.4, 6H, *m*-Ph), 7.12 (t, $^3J_{H–H}$ = 7.4, 3H, *p*-Ph), 7.03 (m, 2H, CH-arom, POP), 6.89 (d, $^3J_{H–H}$ = 7.4, 2H, CH-arom, POP), 6.82 (t, $^3J_{H–H}$ = 7.5, 2H, CH-arom, POP), 2.21 (m, 2H, PC*H*$(CH_3)_2$), 1.38 (s, 3H, C$(CH_3)_2$), 1.13 (dvt, $^3J_{H–H}$ = 7.1, *N* = 15.2, 6H, PCH(C*H*$_3)_2$), 1.04 (s, 3H, C$(CH_3)_2$), 0.98 (dvt, $^3J_{H–H}$ = 7.4, *N* = 16.9, 6H, PCH(C*H*$_3)_2$), 0.77–0.66 (m, 12H, PCH(C*H*$_3)_2$), 0.48 (m, 2H, PC*H*$(CH_3)_2$), –0.12 (t, $^2J_{H–P}$ = 10.3, 1H, OsH), –10.50 (br, 2H, OsH). ^1H NMR (400.13 MHz, toluene-d_8, 203 K, high-field region) δ –0.14 (t, $^3J_{H–H}$ = 9.1, 1H, OsH), –3.73 (br, 1H, OsH), –17.08 (br, 1H, OsH). $^{13}C\{^1H\}$-APT NMR (100.62 MHz, toluene-d_8, 298 K) δ 162.0 (m, C-arom, POP), 149.0 (s, C-ipso, Ph), 138.3 (s, CH, Ph), 134.1 (s, C-arom, POP), 129.2 (s, CH-arom, POP), 128.4 (s, CH-arom, POP), 127.1 (s, CH-arom, POP), 127.0 (m, C-arom, POP), 126.4 (s, CH, Ph), 125.0 (s, CH, Ph), 34.8 (s, *C*$(CH_3)_2$), 31.7 (s, C(*C*$H_3)_2$), 23.0 (vt, *N* = 31.9, P*C*H$(CH_3)_2$), 22.8 (vt, *N* = 24.4, P*C*H$(CH_3)_2$), 22.2 (s, C(*C*$H_3)_2$), 21.2 (s, PCH(*C*$H_3)_2$), 19.6 (s, PCH(*C*$H_3)_2$), 18.5 (m, PCH(*C*$H_3)_2$), 14.7 (s, PCH(*C*$H_3)_2$). $^{31}P\{^1H\}$ NMR (161.98 MHz, toluene-d_8, 298 K) δ 47.4 (s). $^{29}Si\{^1H\}$ NMR (59.63 MHz, C_6D_6, 298 K) δ 1.5 (t, $^2J_{Si–P}$ = 6.0). $T_{1(min)}$ (ms, OsH, 300.13 MHz, toluene-d_8, 230 K) 251 ± 3 (−17.08 ppm).

Preparation of $OsH_3\{SiMe(OSiMe_3)_2\}\{\kappa^3$-*P,O,P*-[xant($P^iPr_2)_2$]} (4). A solution of **1** (200 mg, 0.31 mmol) in toluene (5 mL) was treated with $HSiMe(OSiMe_3)_2$ (171 μL, 0.63 mmol). The resulting mixture was heated at reflux for 16 h. After that time, the mixture was concentrated to dryness to afford a yellowish residue. Addition of methanol (5 mL) caused the precipitation of a

white solid, which was washed with additional methanol (3 x 5 mL) and dried in vacuo. Yield: 245 mg (91%). Anal. Calcd for $C_{34}H_{64}O_3OsP_2Si_3$: C, 47.63; H, 7.52. Found: C, 47.89; H, 7.38. HRMS (*electrospray, m/z*) calcd. for $C_{34}H_{63}O_3OsP_2Si_3$ $[M - H]^+$: 857.3167, found: 857.3180. IR (cm^{-1}) ν(Os–H) 1818 (m). ^{1}H NMR (400.13 MHz, toluene-d_8, 298 K) δ 7.15 (m, 2H, CH-arom, POP), 6.88 (m, 2H, CH-arom, POP), 6.85 (m, 2H, CH-arom, POP), 2.82 (m, 2H, PC*H*$(CH_3)_2$), 2.37 (m, 2H, PC*H*$(CH_3)_2$), 1.38 (dvt, $^3J_{H–H}$ = 7.1, *N* = 17.3, 6H, PCH(C*H*$_3)_2$), 1.34 (s, 3H, C$(CH_3)_2$), 1.14 (dvt, $^3J_{H–H}$ = 5.8, *N* = 12.3, 6H, PCH(C*H*$_3)_2$), 1.08 (dvt, $^3J_{H–H}$ = 7.2, *N* = 16.2, 6H, PCH(C*H*$_3)_2$), 1.05 (dvt, $^3J_{H–H}$ = 6.8, *N* = 15.4, 6H, PCH(C*H*$_3)_2$), 0.94 (s, 3H, C$(CH_3)_2$), 0.74 (s, 3H, SiCH_3), 0.38 (s, 18H, OSi$(CH_3)_3$), –1.34 (tt, $^2J_{H–H}$ = 3.2, $^2J_{H–P}$ = 11.1, 1H, OsH), –11.58 (br, 2H, OsH). ^{1}H NMR (400.13 MHz, toluene-d_8, 203 K, high-field region) δ –1.53 (t, $^2J_{H–P}$ = 10.4, 1H, OsH), –4.42 (br, 1H, OsH), –18.85 (br, 1H, OsH). ^{13}C{^{1}H}-APT NMR (100.62 MHz, toluene-d_8, 298 K) δ 162.2 (vt, *N* = 13.1, C-arom, POP), 134.2 (vt, *N* = 5.3, C-arom, POP), 129.6 (s, CH-arom, POP), 128.8 (s, CH-arom, POP), 127.4 (vt, *N* = 26.2, C-arom, POP), 125.5 (s, CH-arom, POP), 35.2 (s, *C*$(CH_3)_2$), 33.1 (s, C(*C*$H_3)_2$), 27.0 (vt, *N* = 23.4, P*C*H$(CH_3)_2$), 23.5 (vt, *N* = 32.1, P*C*H$(CH_3)_2$), 22.9 (s, C(*C*$H_3)_2$), 21.4 (s, SiCH_3), 19.7 (m, PCH(*C*$H_3)_2$), 16.2 (m, PCH(*C*$H_3)_2$), 3.8 (s, OSi$(CH_3)_3$). ^{31}P{^{1}H} NMR (161.98 MHz, toluene-d_8, 298 K) δ 53.8 (s). ^{29}Si{^{1}H} NMR (59.63 MHz, toluene-d_8, 298 K) δ –8.5 (s, OSi$(CH_3)_3$), –19.8 (t, $^2J_{Si–P}$ = 5.4, SiCH_3). $T_{1(min)}$ (ms, OsH, 300.13 MHz, toluene-d_8, 223 K) 288 ± 3 (−18.85 ppm).

Reaction of $OsH_4\{\kappa^3$-*P*,*O*,*P*-[xant($P^iPr_2)_2$]} (1) with $(Me_3SiO)_2MeSiD$. $(Me_3SiO)_2MeSiD$ (9 μL, 0.032 mmol) was added to a solution of **1** (10 mg, 0.016 mmol) in 0.5 mL of toluene. The mixture was heated at 140 ºC for 18 h. After that the solvent was removed under vacuo. The ^{1}H NMR (300.13 MHz, toluene-d_8, 203 K) data was identical to that reported for **4** except for the

intensity of signals at δ –4.42 (OsH) and –18.85 (OsH), meaning a 50% incorporation of deuterium at hydride positions.

Preparation of $OsH_4\{\kappa^2$-*P,P*-[xant($P^iPr_2)_2$]}(P^iPr_3) (5). A suspension of **1** (200 mg, 0.31 mmol) in methanol (5 mL) was treated with P^iPr_3 (60 μL, 0.31 mmol). The resulting mixture was stirred at room temperature for two days. After that time, a white solid was separated, washed with methanol (3 x 5 mL), and dried under vacuum. Yield: 196 mg (78%). Colorless single crystals suitable for X-ray diffraction analysis were obtained by slow diffusion of pentane into a saturated solution of **5** in benzene at room temperature. Anal. Calcd for $C_{36}H_{65}OOsP_3$: C, 54.25; H, 8.22. Found: C, 54.35; H, 8.39. HRMS (*electrospray, m/z*) calcd. for $C_{36}H_{62}OOsP_3$ $[M - H_2 - H]^+$: 795.3625, found: 795.3614. IR (cm^{-1}) ν(Os–H) 2056 (m), ν(Os–H) 2007 (m), ν(Os–H) 1955 (m). ^{1}H NMR (300.13 MHz, C_6D_6, 298 K) δ 7.18 (m, 2H, CH-arom, POP), 7.11 (m, 2H, CH-arom, POP), 6.99 (m, 2H, CH-arom, POP), 2.55 (m, 4H, PC*H*$(CH_3)_2$, POP), 1.82 (m, 3H, PC*H*$(CH_3)_2$, P^iPr_3), 1.51 (m, 12H, PCH(C*H*$_3)_2$, POP), 1.42 (s, 6H, C$(CH_3)_2$), 1.24 (m, 12H, PCH(C*H*$_3)_2$, POP), 0.93 (dd, $^3J_{H–H}$ = 7.0, $^3J_{H–P}$ = 12.5, 18H, PCH(C*H*$_3)_2$), –10.87 (br, 4H, OsH). ^{1}H NMR (400.13 MHz, toluene-d_8, 235 K, high-field region) δ –9.99 (br, 2H, OsH), –11.90 (br, 2H, OsH). $^{13}C\{^1H\}$-APT NMR (75.47 MHz, C_6D_6, 298 K) δ 156.9 (d, $^2J_{C–P}$ = 6.7, C-arom, POP), 136.0 (d, $^3J_{C–P}$ = 2.6, C-arom, POP), 134.2 (d, $^1J_{C–P}$ = 27.0, C-arom, POP), 128.1 (s, CH-arom, POP), 123.8 (s, CH-arom, POP), 121.8 (d, $^3J_{C–P}$ = 4.1, CH-arom, POP), 36.4 (s, *C*$(CH_3)_2$), 31.1 (d, $^1J_{C–P}$ = 25.1, P*C*H$(CH_3)_2$, P^iPr_3), 20.6 (br, PCH(*C*H$_3)_2$, POP), 20.4 (s, PCH(*C*H$_3)_2$, P^iPr_3), 19.3 (br, PCH(*C*H$_3)_2$, POP), (P*C*H$(CH_3)_2$, POP carbon atoms are not observed at this temperature). $^{31}P\{^1H\}$ NMR (121.49 MHz, C_6D_6, 298 K) δ 44.6 (t, $^2J_{P–P}$ = 66.2, P^iPr_3), 8.4 (br, POP). $^{31}P\{^1H\}$ NMR (161.98 MHz, toluene-d_8, 235 K) δ 44.1 (d, $^2J_{P–P}$ = 129.8, P^iPr_3), 14.7 (d, $^2J_{P–P}$ = 129.6, POP), 2.3 (s, POP). $T_{1(min)}$ (ms, OsH, 300 MHz, toluene-d_8, 253 K) 162 ± 3 (−11.90 ppm).

Preparation of Os{C≡CC(OH)Ph$_2$}$_2${═C═CHC(OH)Ph$_2$}{κ^3-*P,O,P*-[xant(P^{i}Pr$_2$)$_2$]} (6). A solution of **2** (200 mg, 0.27 mmol) in toluene (3 mL) was tretated with 1,1-diphenyl-2-propyn-1-ol (222 mg, 1.07 mmol). The mixture was heated at 80 ºC for 2 h in a Schlenk tube provided with a Teflon closure. The resulting solution was filtered and concentrated to dryness. Addition of pentane (5 mL) afforded a brown precipitate which was washed with pentane (3 x 3 mL) and dried in vacuum. Yield: 174 mg (52%). Brown single crystals suitable for X-ray diffraction analysis were obtained from a saturated methanol solution of **6** at –18 ºC. Anal. Calcd for $C_{72}H_{74}O_4OsP_2$: C, 68.88; H, 5.94. Found: C, 69.05; H, 5.97. HRMS (electrospray, *m/z*) calcd. for $C_{72}H_{75}O_4OsP_2$ $[M + H]^+$: 1257.4758, found: 1257.4733. IR (cm^{-1}) ν(O–H) 3395 (w); ν(C≡C) 2091 (w); ν(C=C) 1655 (m). ^{1}H NMR (400.13 MHz, C_6D_6, 298 K) δ 7.72 (d, $^3J_{H–H}$ = 8.3, 4H, CH-arom), 7.46-7.40 (m, 8H, CH-arom), 7.20 (m, 6H, CH-arom), 7.09 (m, 2H, CH-arom), 6.96-6.91 (m, 12H, CH-arom), 6.84 (m, 4H, CH-arom), 4.61 (s, 1H, (═C═CH–C(O*H*)Ph$_2$), 2.96 (m, 4H, PC*H*(CH$_3$)$_2$), 2.62 (s, 2H, –C≡C–C(OH)Ph$_2$), 2,45 (t, $^4J_{H–P}$ = 2.7, 1H, Os=C=CH), 1.35 (s, 6H, C(C*H*$_3$)$_2$), 1.26 (dvt, $^3J_{H–H}$ = 7.4, *N* = 16.1, 12H, PCH(*CH*$_3$)$_2$), 1.18 (dvt, $^3J_{H–H}$ = 7.1, *N* = 14.8, 12H, PCH(*CH*$_3$)$_2$). ^{13}C{^{1}H}-APT NMR (100.64 MHz, C_6D_6, 298 K) δ 291.6 (t, $^2J_{C–P}$ = 9.1, Os=C), 156.2 (vt, *N* = 11.3, C-arom, POP), 152.1 (s, Os=C=CH–*C*(OH)Ph$_2$), 148.0 (s, C-ipso, Ph), 133.2 (s, CH-arom, POP), 132.3 (vt, *N* = 5.1, C-arom, POP), 129.4 (s, CH-arom, POP), 129.0 (s, CH-arom), 128.5 (vt, *N* = 32.0, C-arom, POP), 127.9 (s, C-arom), 127.8 (s, CH-arom), 127.0 (s, CH-arom), 126.5 (s, CH-arom), 126.4 (s, CH-arom), 126.2 (s, CH-arom), 124.9 (vt, *N* = 5.5, CH-arom, POP), 120.9 (s, C-arom), 111.5 (t, $^3J_{C–P}$ = 3.8, =C=*C*H–C(OH)Ph$_2$), 102.0 (t, $^2J_{C–P}$ = 11.8, Os–*C*≡C), 75.5 (s, Os–C≡*C*), 71.6 (s, =C=CH–*C*(OH)Ph$_2$), 34.5 (s, *C*(CH$_3$)$_2$), 32.0 (s, C(*C*H$_3$)$_2$), 27.4 (vt, *N* = 26.8, P*C*H(CH$_3$)$_2$), 21.8 (s, PCH(*C*H$_3$)$_2$), 19.8 (s, PCH(*C*H$_3$)$_2$). ^{31}P{^{1}H} NMR (161.98 MHz, C_6D_6, 298 K) δ 12.7 (s).

Preparation of Os{C≡CC(OH)Ph$_2$}$_2${=C=C=CPh$_2$}{κ^3-*P,O,P*-[xant(P^{i}Pr$_2$)$_2$]} (7). A suspension of **6** (150 mg, 0.12 mmol) in methanol (5 mL) was stirred at room temperature for 4 h. During this time a green solid precipitated in the media. This solid was washed with additional methanol (3 x 3 mL) and dried in vacuo. Yield: 125 mg (85%). Green single crystals suitable for X-ray diffraction analysis were obtained from a saturated methanol solution of **7** at –18 ºC. Anal. Calcd for $C_{72}H_{72}O_3OsP_2$: C, 69.88; H, 5.86. Found: C, 69.48; H, 6.23. HRMS (electrospray, *m/z*) calcd. for $C_{72}H_{73}O_3OsP_2$ $[M + H]^+$: 1239.4652, found: 1239.4627. IR (cm^{-1}) ν(O–H) 3442 (w); ν(C≡C) 2083 (w); ν(Os=*C*=*C*) 1888 (m). ^{1}H NMR (400.13 MHz, C_6D_6, 298 K) δ 7.83 (d, $^3J_{H–H}$ = 7.3, 4H, CH-arom), 7.38 (d, $^3J_{H–H}$ = 6.7, 8H, CH-arom), 7.24 (m, 2H, CH-arom), 7.17 (m, 2H, CH-arom), 7.05 (t, $^3J_{H–H}$ = 7.7, 4H, CH-arom), 6.93-6.82 (m, 16H, CH-arom), 3.01 (m, 4H, PC*H*(CH$_3$)$_2$), 2.32 (s, 2H, OH), 1.45 (s, 6H, C(C*H*$_3$)$_2$), 1.39 (dvt, $^3J_{H–H}$ = 7.6, *N* = 15.8, 12H, PCH(*CH*$_3$)$_2$), 1.22 (dvt, $^3J_{H–H}$ = 7.0, *N* = 14.2, 12H, PCH(*CH*$_3$)$_2$). ^{13}C{^{1}H}-APT NMR (100.64 MHz, C_6D_6, 298 K) δ 251.3 (t, $^3J_{C–P}$ = 10.1, Os=C=*C*), 247.3 (t, $^2J_{C–P}$ = 3.7, Os=C), 155.8 (vt, *N* = 11.5, C-arom, POP), 154.2 (t, $^4J_{C–P}$ = 2.1, Os=C=C=*C*), 148.8 (s, C-ipso, Ph), 133.8 (s, CH-arom, POP), 131.8 (vt, *N* = 4.8, C-arom, POP), 129.5 (vt, *N* = 30.8, C-arom, POP), 129.4 (s, CH-arom, POP), 129.0 (s, CH-arom), 128.4 (s, C-arom), 127.7 (s, CH-arom), 127.0 (s, CH-arom), 126.9 (s, CH-arom), 126.8 (s, CH-arom), 126.3 (s, CH-arom), 125.4 (t, $^4J_{C–P}$ = 1.2, C(OH)Ph$_2$), 124.6 (vt, *N* = 5.1, CH-arom, POP), 103.8 (t, $^2J_{C–P}$ = 11.7, Os–*C*≡C), 75.1 (s, Os–C≡*C*), 34.4 (s, *C*(CH$_3$)$_2$), 33.9 (s, C(*C*H$_3$)$_2$), 26.9 (vt, *N* = 26.4, P*C*H(CH$_3$)$_2$), 22.1 (s, PCH(*C*H$_3$)$_2$), 19.6 (s, PCH(*C*H$_3$)$_2$). ^{31}P{^{1}H} NMR (161.98 MHz, C_6D_6, 298 K) δ 13.3 (s).

Preparation of OsH{κ^1-C,η^2-[C$_6$H$_4$CH$_2$CH=CH$_2$]}{κ^3-*P,O,P*-[xant(P^{i}Pr$_2$)$_2$]} (8). A solution of **2** (100 mg, 0.13 mmol) in toluene (5 mL) was treated with 1-phenyl-1-propyne (33 μL, 0.27 mmol). This mixture was heated at reflux for 16 h. After that time, the solution was concentrated

to dryness under vacuum. The crude was dissolved in 1 mL of toluene and purified by flash column chromatography charged with neutral alumina and eluted with toluene. The resultant solution was concentrated under vacuum to furnish a yellow solid. Yield: 65 mg (65%). Yellow single crystals suitable for X-ray diffraction analysis were obtained from a saturated methanol solution of **8** at –18 ºC. Anal. Calcd for $C_{36}H_{50}OOsP_2$: C, 57.58; H, 6.71. Found: C, 57.67; H, 6.66. HRMS (*electrospray, m/z*) calcd. for $C_{36}H_{50}OOsP_2$ $[M]^+$: 752.2948, found: 752.2970. IR (cm^{-1}) ν(Os–H) 2040 (w); ν(C=C) 1569 (w). ^{1}H NMR (500.12 MHz, C_6D_6, 298 K) δ 7.97 (d, $^3J_{H-H}$ = 7.3, 1H, CH-arom), 7.22 (ddd, $^3J_{H-H}$ = 1.9, $^3J_{H-P}$ = 5.7, $^3J_{H-H}$ = 7.2, 1H, CH-arom), 7.20-7.13 (m, 3H, CH-arom), 6.92-6.82 (m, 4H, CH-arom), 6.78 (ddd, $^3J_{H-H}$ = 1.5, $^3J_{H-H}$ = 7.3, $^3J_{H-H}$ = 7.3, 1H, CH-arom), 3.84-3.64 (m, 3H, CH_2=C*H*–C*H*$_2$), 2.84 (m, 1H, PC*H*$(CH_3)_2$), 2.78 (m, 1H, PC*H*$(CH_3)_2$), 2.54-2.44 (m, 2H, PC*H*$(CH_3)_2$ + C*H*$_2$=CH), 2.31 (m, 1H, PC*H*$(CH_3)_2$), 1.84 (t, $^3J_{H-H}$ = 6.4, 1H, C*H*$_2$=CH), 1.49 (dd, $^3J_{H-H}$ = 6.8, $^3J_{H-P}$ = 15.5, 3H, PCH(C*H*$_3)_2$), 1.43 (dd, $^3J_{H-H}$ = 6.7, $^3J_{H-P}$ = 16.6, 3H, PCH(C*H*$_3)_2$), 1.30 (s, 3H, C(C*H*$_3)_2$), 1.18 (dd, $^3J_{H-H}$ = 5.7, $^3J_{H-P}$ = 13.6, 3H, PCH(C*H*$_3)_2$), 1.13 (dd, $^3J_{H-H}$ = 7.2, $^3J_{H-P}$ = 13.2, 3H, PCH(C*H*$_3)_2$), 1.09 (dd, $^3J_{H-H}$ = 6.8, $^3J_{H-P}$ = 14.6, 3H, PCH(C*H*$_3)_2$), 1.05 (dd, $^3J_{H-H}$ = 7.0, $^3J_{H-P}$ = 14.1, 3H, PCH(C*H*$_3)_2$), 0.86 (s, 3H, C(C*H*$_3)_2$), 0.73 (dd, $^3J_{H-H}$ = 6.8, $^3J_{H-P}$ = 14.8, 3H, PCH(C*H*$_3)_2$), –7.15 (dd, $^2J_{H-P}$ = 33.0, $^2J_{H-P}$ = 37.4, 1H, OsH). ^{13}C{^{1}H}-APT NMR (125.77 MHz, C_6D_6, 298 K) δ 159.7 (d, $^2J_{C-P}$ = 9.2, C-arom, POP), 158.7 (dd, $^4J_{C-P}$ = 1.2, $^2J_{C-P}$ = 9.5, C-arom, POP), 153.0 (t, $^2J_{C-P}$ = 1.6, Os–C), 145.5 (s, CH, Ph), 141.6 (dd, $^3J_{C-P}$ = 4.1, $^3J_{C-P}$ = 5.9, CH, Ph), 133.7 (d, $^3J_{C-P}$ = 4.7, C-arom, POP), 133.0 (d, $^3J_{C-P}$ = 5.1, C-arom, POP), 130.4 (d, $^3J_{C-P}$ = 29.5, C-arom, POP), 130.0 (s, CH-arom, POP), 129.9 (s, CH-arom, POP), 129.3 (d, $^3J_{C-P}$ = 30.7, C-arom, POP), 125.5 (m, CH-arom, POP), 125.5 (m, CH-arom, POP), 125.3 (s, CH-arom, POP), 125.2 (s, CH-arom, POP), 125.1 (s, CH-arom, POP), 125.0 (m, CH-arom, POP), 123.1 (s, CH, Ph), 122.3 (s, CH, Ph), 118.8 (s, CH, Ph), 42.3 (t,

$^{4}J_{C-P}$ = 1.9, CH_2=CH–CH_2), 41.0 (t, $^{3}J_{C-P}$ = 6.2, CH_2=CH–CH_2), 36.3 (dd, $^{2}J_{C-P}$ = 5.2, $^{2}J_{C-P}$ = 8.5, CH_2=CH), 35.1 (d, $^{2}J_{C-P}$ = 2.3, P$CH(CH_3)_2$), 35.0 (s, $C(CH_3)_2$), 34.9 (m, P$CH(CH_3)_2$), 33.6 (s, C$(CH_3)_2$), 32.8 (d, $^{2}J_{C-P}$ = 2.6, P$CH(CH_3)_2$), 32.7 (d, $^{2}J_{C-P}$ = 2.6, P$CH(CH_3)_2$), 22.9 (s, C$(CH_3)_2$), 22.5 (s, PCH$(CH_3)_2$), 21.2 (d, $^{2}J_{C-P}$ = 6.2, PCH$(CH_3)_2$), 20.7 (s, PCH$(CH_3)_2$), 20.6 (s, PCH$(CH_3)_2$), 20.5 (s, PCH$(CH_3)_2$), 20.3 (d, $^{2}J_{C-P}$ = 4.3, PCH$(CH_3)_2$), 20.1 (d, $^{2}J_{C-P}$ = 5.1, PCH$(CH_3)_2$), 19.6 (d, $^{2}J_{C-P}$ = 3.6, PCH$(CH_3)_2$). $^{31}P\{^{1}H\}$ NMR (202.46 MHz, C_6D_6, 298 K) δ 36.2 (AB spin system, $\Delta\nu$ = 726.1 Hz, J_{A-B} = 164.3 Hz).

Catalytic Dimerization of 1,1-Diphenyl-2-propyn-1-ol to (*Z*)-1,1,6,6-Tetraphenylhex-2-en-4-yne-1,6-diol. An NMR tube was charged with a solution of 1,1-diphenyl-2-propyn-1-ol (55.4 mg, 0.27 mmol) and **2** (10 mg, 0.013 mmol) in toluene-d_8 (0.5 mL). Then, it was placed into a thermostatic bath at 110 ºC and the reaction was monitored by ^{1}H NMR spectroscopy, using 1,4-dioxane (2.8 μL, 0.033 mmol) as internal standard. After 2 h, the ^{1}H NMR spectra of the solution showed conversion to (*Z*)-1,1,6,6-tetraphenylhex-2-en-4-yne-1,6-diol in 70% yield. HRMS (*electrospray, m/z*) calcd. for $C_{30}H_{24}NaO_2$ $[M + Na]^+$: 439.1669, found: 439.1659. IR (cm^{-1}) ν(O–H) 3529 (w); ν(O–H) 3402 (w). ^{1}H NMR (300.13 MHz, $CDCl_3$, 298 K) δ 7.80-7.17 (m, 20H, CH-arom), 6.61 (d, $^{3}J_{H-H}$ = 11.7, 1H, CH=CH), 5.87 (d, $^{3}J_{H-H}$ = 11.7, 1H, CH=CH), 3.55 (s, OH), 2.69 (s, OH). $^{13}C\{^{1}H\}$-APT NMR (75.47 MHz, $CDCl_3$, 298 K) δ 149.6 (s, CH=CH), 146.2 (s, C-arom), 144.5 (s, C-arom), 130.2 (s, CH-arom), 128.4 (s, CH-arom), 127.8 (s, CH-arom), 127.4 (s, CH-arom), 126.9 (s, CH-arom), 126.1 (s, CH-arom), 109.3 (s, CH=CH), 100.9 (s, C≡C), 83.4 (s, C≡C), 79.7 (s, C(OH)Ph_2), 74.8 (s, C(OH)Ph_2).

Catalytic Dimerization of 1,1-Diphenyl-2-propyn-1-ol to (*E*)-2-(5,5-diphenylfuran-2(*5H*)-ylidene)-1,1-diphenylethan-1-ol. An NMR tube was charged with a solution of 1,1-diphenyl-2-propyn-1-ol (55.4 mg, 0.27 mmol) and **2** (10 mg, 0.013 mmol) in toluene-d_8 (0.5 mL). Then, it

was placed into a thermostatic bath at 140 ºC and the reaction was monitored by ^{1}H NMR spectroscopy, using 1,4-dioxane (2.8 μL, 0.033 mmol) as internal standard. After 24 h, the ^{1}H NMR spectra of the solution showed conversion to (*E*)-2-(5,5-diphenylfuran-2(*5H*)-ylidene)-1,1-diphenylethan-1-ol in 80% yield. HRMS (*electrospray, m/z*) calcd. for $C_{30}H_{24}NaO_2$ $[M + Na]^+$: 439.1669, found: 439.1675. IR (cm^{-1}) ν(O–H) 3534 (w). ^{1}H NMR (300.13 MHz, $CDCl_3$, 298 K) δ 7.82-6.97 (m, 20H, CH-arom), 6.63 (d, $^{3}J_{H-H}$ = 5.8, 1H, C*H*=CH), 6.22 (d, $^{3}J_{H-H}$ = 5.8, 1H, CH=C*H*), 5.38 (s, CH=C), 4.35 (s, OH). ^{13}C{^{1}H}-APT NMR (75.47 MHz, $CDCl_3$, 298 K) δ 157.9 (s, CH=*C*), 148.1 (s, C-arom), 142.1 (s, C-arom), 138.3 (s, C*H*=CH), 137.7 (s, C-arom), 128.5 (s, CH-arom), 128.1 (s, CH-arom), 127.9 (s, CH-arom), 126.8 (s, CH-arom), 126.6 (s, CH-arom), 126.4 (s, CH-arom), 124.5 (s, CH=C*H*), 106.6 (s, *C*H=C), 98.4 (s, $C(OH)Ph_2$), 78.1 (s, $C(OH)Ph_2$).

Kinetic Experiments. All kinetic experiments were performed in toluene-d_8 solutions contained in NMR tubes. The NMR tubes were charged with complex **1** (10 mg, 0.016 mmol, 1.9×10^{-2} M) and triethylsilane (49.5–99 μL, 0.31–0.62 mmol, 0.38–0.76 M), the final volume was brought to 850 μL using toluene-d_8, a capillary tube filled with a solution of the internal standard (PPh_3) in toluene-d_8 was also placed in the tube. The reaction was monitored by ^{31}P{^{1}H} NMR spectroscopy every 15 min (a delay of 8 s was used).

ASSOCIATED CONTENT

Supporting Information

The Supporting Information is available free of charge at https://pubs.acs.org/doi/xxxxx.

Experimental details, crystallographic data, theoretical studies, NMR and IR spectra, deuteration and kinetic experiments (PDF).

Cartesian coordinates of the optimized structures (XYZ).

Accession codes

CCDC 2167974-2167978 contain the crystallographic data for this paper. These data can be obtained free of charge via www.ccdc.cam.ac.uk/data_request/cif, or by e-mailing data_request@ccdc.cam.ac.uk, or by contacting The Cambridge Crystallographic Data Centre, 12 Union Road, Cambridge CB2 1EZ, UK; fax: +44 1223 336033

AUTHOR INFORMATION

Corresponding Author

*maester@unizar.es

Notes

The authors declare no competing financial interest.

ACKNOWLEDGMENT

Financial support from the MICIN/AEI/10.13039/501100011033 (PID2020-115286GB-I00 and RED2018-102387-T), Gobierno de Aragón (E06_20R and LMP23_21), FEDER, and the European Social Fund is acknowledged.

REFERENCES

(1) Esteruelas, M. A.; López, A. M.; Oliván, M. Polyhydrides of Platinum Group Metals: Nonclassical Interactions and σ-Bond Activation Reactions. *Chem. Rev.* **2016**, *116*, 8770–8847.

(2) (a) Balcells, D.; Clot, E.; Eisenstein, O. C–H Bond Activation in Transition Metal Species from a Computational Perspective. *Chem. Rev.* **2010**, *110*, 749–823. (b) Eisenstein, O.; Milani, J.; Perutz, R. N. Selectivity of C–H Activation and Competition between C–H and C–F Bond Activation at Fluorocarbons. *Chem. Rev.* **2017**, *117*, 8710–8753. (c) Esteruelas, M. A.; Oliván, M.; Oñate, E. Sigma-bond activation reactions induced by unsaturated Os(IV)-hydride complexes. *Adv. Organomet. Chem.* **2020**, *74*, 53–104.

(3) Corey, J. Y. Reactions of Hydrosilanes with Transition Metal Complexes. *Chem. Rev.* **2016**, *116*, 11291–11435.

(4) (a) Buil, M. L.; Espinet, P.; Esteruelas, M. A.; Lahoz, F. J.; Lledós, A.; Martínez-Ilarduya, J. M.; Maseras, F.; Modrego, J.; Oñate, E.; Oro, L. A.; Sola, E.; Valero, C. Oxidative Addition of Group 14 Element Hydrido Compounds to $OsH_2(\eta^2\text{-}CH_2{=}CHEt)(CO)(P^iPr_3)_2$: Synthesis and Characterization of the First Trihydrido–Silyl, Trihydrido–Germyl, and Trihydrido–Stannyl Derivatives of Osmium(IV). *Inorg. Chem.* **1996**, *35*, 1250–1256. (b) Hübler, K.; Hübler, U.; Roper, W. R.; Schwerdtfeger, P.; Wright, L. J. The Nature of the Metal–Silicon Bond in $[M(SiR_3)H_3(PPh_3)_3]$ (M = Ru, Os) and the Crystal Structure of $[Os\{Si(N\text{-pyrrolyl})_3\}H_3(PPh_3)_3]$. *Chem. Eur. J.* **1997**, *3*, 1608–1616. (c) Möhlen, M.; Rickard, C. E. F.; Roper, W. R.; Salter, D. M.; Wright, L. J. The synthesis, structure, and reactivity of the osmium(IV) trihydrido silyl complex, $OsH_3(SiMe_3)(CO)(PPh_3)_2$. *J. Organomet. Chem.* **2000**, *593–594*, 458–464. (d) Rickard, C. E. F.; Roper, W. R.; Woodgate, S. D.; Wright, L. J. Silatranyl, hydride complexes of osmium(II) and

osmium(IV): crystal structure of $Os(Si\{OCH_2CH_2\}_3N)H_3(PPh_3)_3$. *J. Organomet. Chem.* **2000**, *609*, 177–183. (e) Gusev, D. G.; Fontaine, F.-G.; Lough, A. J.; Zargarian, D. Polyhydrido(silylene)osmium and Silyl(dinitrogen)ruthenium Products Through Redistribution of Phenylsilane with Osmium and Ruthenium Pincer Complexes. *Angew. Chem., Int. Ed.* **2003**, *42*, 216–219. (f) He, G.; Wu, L.; Bai, W.; Chen, J.; Sung, H. H. Y.; Williams, I. D.; Lin, Z.; Jia, G. Synthesis and Reactivities of Polyhydrido Osmium Arylsilyl Complexes Prepared from $OsH_3Cl(PPh_3)_3$. *Organometallics* **2017**, *36*, 3729–3738.

(5) (a) Gilbert, T. M.; Hollander, F. J.; Bergman, R. G. (Pentamethylcyclopentadienyl)iridium Polyhydride Complexes: Synthesis of Intermediates in the Mechanism of Formation of $(C_5(CH_3)_5)IrH_4$ and the Preparation of Several Iridium(V) Compounds. *J. Am. Chem. Soc.* **1985**, *107*, 3508–3516. (b) Loza, M.; Faller, J. W.; Crabtree, R. H. Seven-Coordinate Iridium(V) Polyhydrides with Chelating Bis(silyl) Ligands. *Inorg. Chem.* **1995**, *34*, 2937–2941. (c) Gutiérrez-Puebla, E.; Monge, A.; Paneque, M.; Poveda, M. L.; Taboada, S.; Trujillo, M.; Carmona, E. Synthesis and Properties of $Tp^{Me2}IrH_4$ and $Tp^{Me2}IrH_3(SiEt_3)$: Ir(V) Polyhydride Species with C_{3v} Geometry. *J. Am. Chem. Soc.* **1999**, *121*, 346–354. (d) Turculet, L.; Feldman, J. D.; Tilley, T. D. Coordination Chemistry and Reactivity of New Zwitterionic Rhodium and Iridium Complexes Featuring the Tripodal Phosphine Ligand $[PhB(CH_2P^iPr_2)_3]^-$. Activation of H–H, Si–H, and Ligand B–C Bonds. *Organometallics* **2004**, *23*, 2488–2502. (e) Esteruelas, M. A.; Fernández-Alvarez, F. J.; López, A. M.; Oñate, E.; Ruiz-Sánchez, P. Iridium(I), Iridium(III), and Iridium(V) Complexes Containing the (2-Methoxyethyl)cyclopentadienyl Ligand. *Organometallics* **2006**, *25*, 5131–5138. (f) Park, S.; Brookhart, M. Development and Mechanistic Investigation of a Highly Efficient Iridium(V) Silyl Complex for the Reduction of Tertiary Amides to Amines. *J. Am. Chem. Soc.* **2012**, *134*, 640–653.

(6) (a) Nikonov, G. I. Recent Advances in Nonclassical Interligand Si···H Interactions. *Adv. Organomet. Chem.* **2005**, *53*, 217-309. (b) Lachaize, S.; Sabo-Etienne, S. σ-Silane Ruthenium Complexes: The Crucial Role of Secondary Interactions. *Eur. J. Inorg. Chem.* **2006**, 2115–2127.

(7) (a) Esteruelas, M. A.; Herrero, J.; López, F. M.; Martín, M.; Oro, L. A. Dehalogenation of Polychloroarenes with $HSiEt_3$ Catalyzed by an Homogeneous Rhodium−Triphenylphosphine System. *Organometallics* **1999**, *18*, 1110–1112. (b) Díaz, J.; Esteruelas, M. A.; Herrero, J.; Moralejo, L.; Oliván, M. Simultaneous Dehalogenation of Polychloroarenes and Chlorination of $HSiEt_3$ Catalyzed by Complexes of the Groups 8 and 9. *J. Catal.* **2000**, *195*, 187–192. (c) Esteruelas, M. A.; Herrero, J.; Oliván, M. Dehalogenation of Hexachlorocyclohexanes and Simultaneous Chlorination of Triethylsilane Catalyzed by Rhodium and Ruthenium Complexes. *Organometallics* **2004**, *23*, 3891–3897.

(8) (a) Corbin, R. A.; Ison, E. A.; Abu-Omar, M. M. Catalysis by cationic oxorhenium(v): hydrolysis and alcoholysis of organic silanes. *Dalton Trans.* **2009**, 2850–2855. (b) Tan, S. T.; Kee, J. W.; Fan, W. Y. Catalytic Hydrogen Generation from the Hydrolysis of Silanes by Ruthenium Complexes. *Organometallics* **2011**, *30*, 4008–4013. (c) Yu, M.; Jing, H.; Fu, X. Highly Efficient Generation of Hydrogen from the Hydrolysis of Silanes Catalyzed by $[RhCl(CO)_2]_2$. *Inorg. Chem.* **2013**, *52*, 10741–10743. (d) Esteruelas, M. A.; Oliván, M.; Vélez, A. POP-Pincer Silyl Complexes of Group 9: Rhodium versus Iridium. *Inorg. Chem.* **2013**, *52*, 12108–12119. (e) Wang, W.; Wang, J.; Huang, L.; Wei, H. Mechanistic insights into hydrogen generation for catalytic hydrolysis and alcoholysis of silanes with high-valent oxorhenium(v) complexes. *Catal. Sci. Technol.* **2015**, *5*, 2157–2166.

(9) Marciniec, B.; Maciejewski, H., Pietraszuk, C.; Pawluć, P.; *Hydrosilylation: Advances In Silicon Science*, vol 1; Marciniec, B., Ed.; Springer: Dordrecht, 2009.

(10) He, P.; Hu, M.-Y.; Zhang, X.-Y.; Zhu, S.-F. Transition-Metal-Catalyzed Stereo- and Regioselective Hydrosilylation of Unsymmetrical Alkynes. *Synthesis* **2022**, *54*, 49–66.

(11) *Modern Alkyne Chemistry: Catalytic and Atom-Economic Transformations*; Trost, B. M,; Li, C-J.; Eds.; Wiley: Weinheim, Germany, 2015.

(12) (a) Esteruelas, M. A.; López, A. M.; Oliván, M. Osmium–carbon double bonds: Formation and reactions. *Coord. Chem. Rev.* **2007**, *251*, 795–840. (b) Castro-Rodrigo, R.; Esteruelas, M. A.; López, A. M.; Oñate, E. Reactions of a Dihydrogen Complex with Terminal Alkynes: Formation of Osmium–Carbyne and –Carbene Derivatives with the Hydridotris(pyrazolyl)borate Ligand. *Organometallics* **2008**, *27*, 3547–3555. (c) Bolaño, T.; Esteruelas, M. A.; Oñate, E. Osmium–carbon multiple bonds: Reduction and C–C coupling reactions. *J. Organomet. Chem.* **2011**, *696*, 3911–3923. (d) Casanova, N.; Esteruelas, M. A.; Gulías, M.; Larramona, C.; Mascareñas, J. L.; Oñate, E. Amide-Directed Formation of Five-Coordinate Osmium Alkylidenes from Alkynes. *Organometallics* **2016**, *35*, 91–99.

(13) Chen, D.; Hua, Y.; Xia, H. Metallaaromatic Chemistry: History and Development. *Chem. Rev.* **2020**, *120*, 12994–13086.

(14) Esteruelas, M. A.; López, A. M. Ruthenium- and Osmium-Hydride Compounds Containing Triisopropylphosphine as Precursors for Carbon-Carbon and Carbon-Heteroatom Coupling Reactions, in *Recent Advances in Hydride Chemistry*; Peruzzini, M., Poli, R., Eds.; Elsevier: Amsterdam, 2001; Chapter 7, pp 189-248.

(15) (a) Werner, H.; Meyer, U.; Esteruelas, M. A.; Sola, E.; Oro, L. A. Bis-alkynyl- and hydrido-alkynyl-osmium(II) and ruthenium(II) complexes containing triisopropylphosphine as ligand. *J. Organomet. Chem.* **1989**, *366*, 187–196. (b) Esteruelas, M. A.; Oro, L. A.; Ruiz, N. Reactions of Osmium Hydride Complexes with Terminal Alkynes: Synthesis and Catalytic Activity of $OsH(\eta^2\text{-}O_2CCH_3)(C{=}CHPh)(P^iPr_3)_2$. *Organometallics* **1994**, *13*, 1507–1509. (c) Yi, C. S.; Liu, N. Homogeneous Catalytic Dimerization of Terminal Alkynes by $C_5Me_5Ru(L)H_3$ (L = PPh_3, PCy_3, PMe_3). *Organometallics* **1996**, *15*, 3968–3971. (d) Esteruelas, M. A.; Herrero, J.; López, A. M.; Oliván, M. Alkyne-Coupling Reactions Catalyzed by $OsHCl(CO)(P^iPr_3)_2$ in the Presence of Diethylamine. *Organometallics* **2001**, *20*, 3202–3205. (e) Gorgas, N.; Alves, L. G.; Stöger, B.; Martins, A. M.; Veiros, L. F.; Kirchner, K. Stable, Yet Highly Reactive Nonclassical Iron(II) Polyhydride Pincer Complexes: *Z*-Selective Dimerization and Hydroboration of Terminal Alkynes. *J. Am. Chem. Soc.* **2017**, *139*, 8130–8133. (f) Gorgas, N.; Stöger, B.; Veiros, L. F.; Kirchner, K. Iron(II) Bis(acetylide) Complexes as Key Intermediates in the Catalytic Hydrofunctionalization of Terminal Alkynes. *ACS Catal.* **2018**, *8*, 7973–7982.

(16) (a) Garcia-Garrido, S. E. Catalytic Dimerization of Alkynes, in *Modern Alkyne Chemistry*; Trost, B. M.; Li, C.-J., Eds.; Wiley: Wenheim, Germany, 2015, pp 301-334. (b) Trost, B. M.; Masters, J. T. Transition metal-catalyzed couplings of alkynes to 1,3-enynes: modern methods and synthetic applications. *Chem. Soc. Rev.* **2016**, *45*, 2212–2238.

(17) Qian, H.; Huang, D.; Bi, Y.; Yan, G. 2-Propargyl Alcohols in Organic Synthesis. *Adv. Synth. Catal.* **2019**, *361*, 3240–3280.

(18) Cadierno, V.; Gimeno, J. Allenylidene and Higher Cumulenylidene Complexes. *Chem. Rev.* **2009**, *109*, 3512–3560.

(19) (a) Kumar, A.; Bhatti, T. M.; Goldman, A. S. Dehydrogenation of Alkanes and Aliphatic Groups by Pincer-Ligated Metal Complexes. *Chem. Rev.* **2017**, *117*, 12357–12384. (b) *Pincer Compounds*; Morales-Morales, D., Ed.; Elsevier, 2018. (c) Valdés, H.; García-Eleno, M. A.; Canseco-Gonzalez, D.; Morales-Morales, D. Recent Advances in Catalysis with Transition-Metal Pincer Compounds. *ChemCatChem* **2018**, *10*, 3136–3172.

(20) (a) Pawley, R. J.; Moxham, G. L.; Dallanegra, R.; Chaplin, A. B.; Brayshaw, S. K.; Weller, A. S.; Willis, M. C. Controlling Selectivity in Intermolecular Alkene or Aldehyde Hydroacylation Reactions Catalyzed by $\{Rh(L_2)\}^+$ Fragments. *Organometallics* **2010**, *29*, 1717–1728. (b) Pontiggia, A. J.; Chaplin, A. B.; Weller, A. S. Cationic iridium complexes of the Xantphos ligand. Flexible coordination modes and the isolation of the hydride insertion product with an alkene. *J. Organomet. Chem.* **2011**, *696*, 2870–2876. (c) Dallanegra, R.; Chaplin, A. B.; Weller, A. S. Rhodium Cyclopentyl Phosphine Complexes of Wide-Bite-Angle Ligands DPEphos and Xantphos. *Organometallics* **2012**, *31*, 2720–2728. (d) Johnson, H. C.; Leitao, E. M.; Whittell, G. R.; Manners, I.; Lloyd-Jones, G. C.; Weller, A. S. Mechanistic Studies of the Dehydrocoupling and Dehydropolymerization of Amine-Boranes Using a $[Rh(Xantphos)]^+$ Catalyst. *J. Am. Chem. Soc.* **2014**, *136*, 9078–9093. (e) Ren, P.; Pike, S. D.; Pernik, I.; Weller, A. S.; Willis, M. C. Rh–POP Pincer Xantphos Complexes for C–S and C–H Activation. Implications for Carbothiolation Catalysis. *Organometallics* **2015**, *34*, 711–723. (f) Barwick-Silk, J.; Hardy, S.; Willis, M. C.; Weller, A. S. Rh(DPEPhos)-Catalyzed Alkyne Hydroacylation Using *β*-Carbonyl-Substituted Aldehydes: Mechanistic Insight Leads to Low Catalyst Loadings that Enables Selective Catalysis on Gram-Scale. *J. Am. Chem. Soc.* **2018**, *140*, 7347–7357. (g) Adams, G. M.; Ryan, D. E.; Beattie, N. A.; McKay, A. I.; Lloyd-Jones, G. C.; Weller, A. S. Dehydropolymerization of $H_3B{\cdot}NMeH_2$ Using a $[Rh(DPEphos)]^+$ Catalyst: The Promoting Effect of $NMeH_2$. *ACS Catal.* **2019**, *9*, 3657–

3666. (h) Dietz, M.; Johnson, A.; Martínez-Martínez, A.; Weller, A. S. The [Rh(Xantphos)]$^{+}$ catalyzed hydroboration of diphenylacetylene using trimethylamine-borane. *Inorganica Chim. Acta* **2019**, *491*, 9–13. (i) Ryan, D. E.; Andrea, K. A.; Race, J. J.; Boyd, T. M.; Lloyd-Jones, G. C.; Weller, A. S. Amine-Borane Dehydropolymerization Using Rh-Based Precatalysts: Resting State, Chain Control, and Efficient Polymer Synthesis. *ACS Catal.* **2020**, *10*, 7443–7448.

(21) (a) Asensio, G.; Cuenca, A. B.; Esteruelas, M. A.; Medio-Simón, M.; Oliván, M.; Valencia, M. Osmium(III) Complexes with POP Pincer Ligands: Preparation from Commercially Available $OsCl_3 \cdot 3H_2O$ and Their X-ray Structures. *Inorg. Chem.* **2010**, *49*, 8665–8667. (b) Esteruelas, M. A.; Oliván, M. Osmium Complexes with POP Pincer Ligands, in *Pincer Compounds*; Morales-Morales, D., Ed.; Elsevier, 2018; Chapter 16, pp 341−357. (c) Curto, S. G.; de las Heras, L. A.; Esteruelas, M. A.; Oliván, M.; Oñate, E.; Vélez, A. Reactions of POP-pincer rhodium(I)-aryl complexes with small molecules: coordination flexibility of the ether diphosphine. *Can. J. Chem.* **2021**, *99*, 127–136.

(22) (a) Esteruelas, M. A.; Oliván, M.; Vélez, A. Xantphos-Type Complexes of Group 9: Rhodium versus Iridium. *Inorg. Chem.* **2013**, *52*, 5339–5349. (b) Alós, J.; Bolaño, T.; Esteruelas, M. A.; Oliván, M.; Oñate, E.; Valencia, M. POP–Pincer Ruthenium Complexes: d^6 Counterparts of Osmium d^4 Species. *Inorg. Chem.* **2014**, *53*, 1195–1209. (c) Esteruelas, M. A.; Oliván, M.; Vélez, A. Conclusive Evidence on the Mechanism of the Rhodium-Mediated Decyanative Borylation. *J. Am. Chem. Soc.* **2015**, *137*, 12321–12329. (d) Esteruelas, M. A.; Oliván, M.; Vélez, A. POP–Rhodium-Promoted C–H and B–H Bond Activation and C–B Bond Formation. *Organometallics* **2015**, *34*, 1911–1924. (e) Alós, J.; Esteruelas, M. A.; Oliván, M.; Oñate, E.; Puylaert, P. C–H Bond Activation Reactions in Ketones and Aldehydes Promoted by POP-Pincer Osmium and Ruthenium Complexes. *Organometallics* **2015**, *34*, 4908–4921. (f) Esteruelas, M.

A.; Fernández, I.; García-Yebra, C.; Martín, J.; Oñate, E. Elongated *σ*-Borane versus *σ*-Borane in Pincer–POP–Osmium Complexes. *Organometallics* **2017**, *36*, 2298–2307. (g) Curto, S. G.; Esteruelas, M. A.; Oliván, M.; Oñate, E.; Vélez, A. Selective C–Cl Bond Oxidative Addition of Chloroarenes to a POP–Rhodium Complex. *Organometallics* **2017**, *36*, 114–128. (h) Curto, S. G.; Esteruelas, M. A.; Oliván, M.; Oñate, E.; Vélez, A. *β*-Borylalkenyl *Z–E* Isomerization in Rhodium-Mediated Diboration of Nonfunctionalized Internal Alkynes. *Organometallics* **2018**, *37*, 1970–1978. (i) Esteruelas, M. A.; Fernández, I.; Martínez, A.; Oliván, M.; Oñate, E.; Vélez, A. Iridium-Promoted B–B Bond Activation: Preparation and X-ray Diffraction Analysis of a *mer*-Tris(boryl) Complex. *Inorg. Chem.* **2019**, *58*, 4712–4717. (j) Esteruelas, M. A.; Fernández, I.; García-Yebra, C.; Martín, J.; Oñate, E. Cycloosmathioborane Compounds: Other Manifestations of the Hückel Aromaticity. *Inorg. Chem.* **2019**, *58*, 2265–2269. (k) Curto, S. G.; de las Heras, L. A.; Esteruelas, M. A.; Oliván, M.; Oñate, E. C(sp^3)–Cl Bond Activation Promoted by a POP-Pincer Rhodium(I) Complex. *Organometallics* **2019**, *38*, 3074–3083. (l) Curto, S. G.; Esteruelas, M. A.; Oliván, M.; Oñate, E. Insertion of Diphenylacetylene into Rh–Hydride and Rh–Boryl Bonds: Influence of the Boryl on the Behavior of the *β*-Borylalkenyl Ligand. *Organometallics* **2019**, *38*, 4183–4192. (m) Esteruelas, M. A.; Martínez, A.; Oliván, M.; Oñate, E. Direct C−H Borylation of Arenes Catalyzed by Saturated Hydride-Boryl-Iridium-POP Complexes: Kinetic Analysis of the Elemental Steps. *Chem. Eur. J.* **2020**, *26*, 12632–12644. (n) de las Heras, L. A.; Esteruelas, M. A.; Oliván, M.; Oñate, E. C–Cl Oxidative Addition and C–C Reductive Elimination Reactions in the Context of the Rhodium-Promoted Direct Arylation. *Organometallics* **2022**, *41*, 716–732.

(23) (a) Esteruelas, M. A.; García-Yebra, C.; Martín, J.; Oñate, E. *mer*, *fac*, and Bidentate Coordination of an Alkyl-POP Ligand in the Chemistry of Nonclassical Osmium Hydrides. *Inorg. Chem.* **2017**, *56*, 676–683. (b) Esteruelas, M.; Oñate, E.; Paz, S.; Vélez, A. Repercussion of a 1,3-

Hydrogen Shift in a Hydride-Osmium-Allenylidene Complex. *Organometallics* **2021**, *40*, 1523–1537.

(24) (a) Alós, J.; Bolaño, T.; Esteruelas, M. A.; Oliván, M.; Oñate, E.; Valencia, M. POP-Pincer Osmium-Polyhydrides: Head-to-Head (*Z*)-Dimerization of Terminal Alkynes. *Inorg. Chem.* **2013**, *52*, 6199–6213. (b) Esteruelas, M. A.; Nolis, P.; Oliván, M.; Oñate, E.; Vallribera, A.; Vélez, A. Ammonia Borane Dehydrogenation Promoted by a Pincer-Square-Planar Rhodium(I) Monohydride: A Stepwise Hydrogen Transfer from the Substrate to the Catalyst. *Inorg. Chem.* **2016**, *55*, 7176–7181. (c) Antiñolo, A.; Esteruelas, M. A.; García-Yebra, C.; Martín, J.; Oñate, E.; Ramos, A. Reactions of an Osmium(IV)-Hydroxo Complex with Amino-Boranes: Formation of Boroxide Derivatives. *Organometallics* **2019**, *38*, 310–318. (d) Curto, S. G.; Esteruelas, M. A.; Oliván, M.; Oñate, E. Rhodium-Mediated Dehydrogenative Borylation–Hydroborylation of Bis(alkyl)alkynes: Intermediates and Mechanism. *Organometallics* **2019**, *38*, 2062–2074. (e) Esteruelas, M. A.; Martínez, A.; Oliván, M.; Oñate, E. Kinetic Analysis and Sequencing of Si–H and C–H Bond Activation Reactions: Direct Silylation of Arenes Catalyzed by an Iridium-Polyhydride. *J. Am. Chem. Soc.* **2020**, *142*, 19119–19131.

(25) (a) Bakhmutov, V. I.; Bozoglian, F.; Gómez, K.; González, G.; Grushin, V. V.; Macgregor, S. A.; Martin, E.; Miloserdov, F. M.; Novikov, M. A.; Panetier, J. A.; Romashov, L. V. CF_3−Ph Reductive Elimination from [(Xantphos)Pd(CF_3)(Ph)]. *Organometallics* **2012**, *31*, 1315–1328. (b) Jover, J.; Miloserdov, F. M.; Benet-Buchholz, J.; Grushin, V. V.; Maseras, F. On the Feasibility of Nickel-Catalyzed Trifluoromethylation of Aryl Halides. Organometallics **2014**, *33*, 6531–6543.

(26) (a) Haibach, M. C.; Wang, D. Y.; Emge, T. J.; Krogh-Jespersen, K.; Goldman, A. S. (POP)Rh pincer hydride complexes: unusual reactivity and selectivity in oxidative addition and

olefin insertion reactions. *Chem. Sci.* **2013**, *4*, 3683–3692. (b) Esteruelas, M. A.; García-Yebra, C.; Martín, J.; Oñate, E. Dehydrogenation of Formic Acid Promoted by a Trihydride-Hydroxo-Osmium(IV) Complex: Kinetics and Mechanism. *ACS Catal.* **2018**, *8*, 11314–11323. (c) Esteruelas, M. A.; Martínez, A.; Oliván, M.; Vélez, A. A General Rhodium Catalyst for the Deuteration of Boranes and Hydrides of the Group 14 Elements. *J. Org. Chem.* **2020**, *85*, 15693–15698.

(27) Buil, M. L.; Esteruelas, M. A.; Fernández, I.; Izquierdo, S.; Oñate, E. Cationic Dihydride Boryl and Dihydride Silyl Osmium(IV) NHC Complexes: A Marked Diagonal Relationship. *Organometallics* **2013**, *32*, 2744–2752.

(28) The separations between the hydrides were calculated from the equation $r_{(H–H)} = 5.815(T_{1(min)}\nu^{-1})^{1/6}$ ($T_{1(min)}$ in s and ν in MHz), assuming slow rotation of the dihydride pair. See: Bautista, M. T.; Cappellani, E. P.; Drouin, S. D.; Morris, R. H.; Schweitzer, C. T.; Sella, A.; Zubkowski, J. Preparation and Spectroscopic Properties of the η^2-Dihydrogen Complexes $[MH(\eta^2\text{-}H_2)(PR_2CH_2CH_2PR_2)_2]^+$ (M = Fe, Ru; R = Ph, Et) and Trends in Properties down the Iron Group Triad. *J. Am. Chem. Soc.* **1991**, *113*, 4876–4887.

(29) Esteruelas, M. A.; López, A. M.; Oñate, E.; Raga, E. Metathesis between E−C(sp^n) and H−C(sp^3) σ-Bonds (E=Si, Ge; n=2, 3) on an Osmium-Polyhydride. *Angew. Chemie Int. Ed.* https://doi.org/10.1002/anie.202204081.

(30) Hart, D. W.; Bau, R.; Koetzle, T. F. Neutron and X-Ray Diffraction Studies on Tris(dimethylphenylphosphine)osmium Tetrahydride. *J. Am. Chem. Soc.* **1977**, *99*, 7557–7564.

(31) Villafañe, F. Dynamic behavior in solution of seven-coordinated transition metal complexes. *Coord. Chem. Rev.* **2014**, *281*, 86–99.

(32) Gómez-Gallego, M.; Sierra, M. A. Kinetic Isotope Effects in the Study of Organometallic Reaction Mechanisms. *Chem. Rev.* **2011**, *111*, 4857–4963.

(33) (a) Buil, M. L.; Esteruelas, M. A.; Garcés, K.; Oñate, E. From Tetrahydroborate– to Aminoborylvinylidene–Osmium Complexes via Alkynyl–Aminoboryl Intermediates. *J. Am. Chem. Soc.* **2011**, *133*, 2250–2263. (b) Esteruelas, M. A.; López, A. M.; Mora, M.; Oñate, E. Reactions of Osmium–Pinacolboryl Complexes: Preparation of the First Vinylideneboronate Esters. *Organometallics* **2012**, *31*, 2965–2970. (c) Buil, M. L.; Cardo, J. J. F.; Esteruelas, M. A.; Oñate, E. Square-Planar Alkylidyne–Osmium and Five-Coordinate Alkylidene–Osmium Complexes: Controlling the Transformation from Hydride-Alkylidyne to Alkylidene. *J. Am. Chem. Soc.* **2016**, *138*, 9720–9728.

(34) Nast, R. Coordination Chemistry of Metal Alkynyl Compounds. *Coord. Chem. Rev.* **1982**, *47*, 89–124.

(35) (a) Barrio, P.; Esteruelas, M. A.; Oñate, E. Reactions of an Osmium-Elongated Dihydrogen Complex with Terminal Alkynes: Formation of Novel Bifunctional Compounds with Amphoteric Nature. *Organometallics* **2002**, *21*, 2491–2503. (b) Barrio, P.; Esteruelas, M. A.; Oñate, E. Reactions of Elongated Dihydrogen-Osmium Complexes Containing Orthometalated Ketones with Alkynes: Hydride-Vinylidene-π-Alkyne versus Hydride-Osmacyclopropene. *Organometallics* **2003**, *22*, 2472–2485. (c) Batuecas, M.; Escalante, L.; Esteruelas, M. A.; García-Yebra, C.; Oñate, E.; Saá, C. Dehydrative Cyclization of Alkynals: Vinylidene Complexes with the C_β Incorporated into Unsaturated Five- or Six-Membered Rings. *Angew. Chem., Int. Ed.* **2011**, *50*, 9712–9715. (d) Müller, A. L.; Wadepohl, H.; Gade, L. H. Bis(pyridylimino)isoindolato (BPI) Osmium Complexes: Structural Chemistry and Reactivity. *Organometallics* **2015**, *34*, 2810–2818.

(e) Wen, T. B.; Lee, K.-H.; Chen, J.; Hung, W. Y.; Bai, W.; Li, H.; Sung, H. H. Y.; Williams, I. D.; Lin, Z.; Jia, G. Preparation of Osmium η^3-Allenylcarbene Complexes and Their Uses for the Syntheses of Osmabenzyne Complexes. *Organometallics* **2016**, *35*, 1514–1525. (f) Esteruelas, M. A.; Gay, M. P.; Oñate, E. Conceptual Extension of the Degradation–Transformation of N-Heterocyclic Carbenes: Unusual Rearrangements on Osmium. *Organometallics* **2018**, *37*, 3412–3424.

(36) (a) Cadierno, V.; Gamasa, M. P.; Gimeno, J.; González-Cueva, M.; Lastra, E.; Borge, J.; García-Granda, S.; Pérez-Carreño, E. Activation of 2-Propyn-1-ol Derivatives by Indenylruthenium(II) and -osmium(II) Complexes: X-ray Crystal Structures of the Allenylidene Complexes $[M(=C=C=CPh_2)(\eta^5\text{-}C_9H_7)(PPh_3)_2][PF_6]\cdot CH_2Cl_2$ (M = Ru, Os) and EHMO Calculations. *Organometallics* **1996**, *15*, 2137–2147. (b) Bohanna, C.; Callejas, B.; Edwards, A. J.; Esteruelas, M. A.; Lahoz, F. J.; Oro, L. A.; Ruiz, N.; Valero, C. The Five-Coordinate Hydrido–Dihydrogen Complex $[OsH(\eta^2\text{-}H_2)(CO)(P^iPr_3)_2]BF_4$ Acting as a Template for the Carbon–Carbon Coupling between Methyl Propiolate and 1,1-Diphenyl-2-propyn-1-ol. *Organometallics* **1998**, *17*, 373–381. (c) Crochet, P.; Esteruelas, M. A.; López, A. M.; Ruiz, N.; Tolosa, J. I. New Cyclopentadienylosmium Compounds Containing Unsaturated Carbon Donor Coligands: Synthesis, Structure, and Reactivity of $Os(\eta^5\text{-}C_5H_5)Cl(=C=C=CPh_2)(P^iPr_3)$. *Organometallics* **1998**, *17*, 3479–3486. (d) Xia, H. P.; Ng, W. S.; Ye, J. S.; Li, X.-Y.; Wong, W. T.; Lin, Z.; Yang, C.; Jia, G. Synthesis and Electrochemical Properties of C_5H–Bridged Bimetallic Iron, Ruthenium, and Osmium Complexes. *Organometallics* **1999**, *18*, 4552–4557. (e) Wen, T. B.; Zhou, Z. Y.; Lo, M. F.; Williams, I. D.; Jia, G. Vinylidene, Allenylidene, and Carbyne Complexes from the Reactions of $[OsCl_2(PPh_3)_3]$ with $HC{\equiv}CC(OH)Ph_2$. *Organometallics* **2003**, *22*, 5217–5225. (f) Asensio, A.; Buil, M. L.; Esteruelas, M. A.; Oñate, E. A Four-Electron π-Alkyne Complex as

Precursor for Allenylidene Derivatives: Preparation, Structure, and Reactivity of [Os(η^5-C_5H_5)(C=C=CPh_2)L(P^{i}Pr_3)]PF_6 (L = CO, PHPh_2). *Organometallics* **2004**, *23*, 5787–5798. (g) Bolaño, T.; Castarlenas, R.; Esteruelas, M. A.; Oñate, E. Assembly of an Allenylidene Ligand, a Terminal Alkyne, and an Acetonitrile Molecule: Formation of Osmacyclopentapyrrole Derivatives. *J. Am. Chem. Soc.* **2006**, *128*, 3965–3973.

(37) Trost, B. M.; McIntosh, M. C. Directing Tandem Catalyzed Reactions as an Approach to Furans and Butenolides. *J. Am. Chem. Soc.* **1995**, *117*, 7255–7256.

(38) (a) Katagiri, T.; Tsurugi, H.; Satoh, T.; Miura, M. Rhodium-catalyzed (*E*)-selective cross-dimerization of terminal alkynes. *Chem. Commun.* **2008**, 3405–3407. (b) Braga, D.; Jaafari, A.; Miozzo, L.; Moret, M.; Rizzato, S.; Papagni, A.; Yassar, A. The Rubrenic Synthesis: The Delicate Equilibrium between Tetracene and Cyclobutene. *European J. Org. Chem.* **2011**, 4160–4169. (c) Zatolochnaya, O. V.; Gordeev, E. G.; Jahier, C.; Ananikov, V. P.; Gevorgyan, V. Carboxylate Switch between Hydro- and Carbopalladation Pathways in Regiodivergent Dimerization of Alkynes. *Chem. Eur. J.* **2014**, *20*, 9578–9588. (d) Ueda, Y.; Tsurugi, H.; Mashima, K. Cobalt-Catalyzed *E*-Selective Cross-Dimerization of Terminal Alkynes: A Mechanism Involving Cobalt(0/II) Redox Cycles. *Angew. Chem., Int. Ed.* **2020**, *59*, 1552–1556.

(39) (a) Liang, Q.; Osten, K. M.; Song, D. Iron-Catalyzed *gem*-Specific Dimerization of Terminal Alkynes. *Angew. Chem., Int. Ed.* **2017**, *56*, 6317–6320. (b) Liang, Q.; Sheng, K.; Salmon, A.; Zhou, V. Y.; Song, D. Active Iron(II) Catalysts toward *gem*-Specific Dimerization of Terminal Alkynes. *ACS Catal.* **2019**, *9*, 810–818.

(40) Nguyen, H. N.; Tashima, N.; Ikariya, T.; Kuwata, S. Ruthenium-Catalyzed Dimerization of 1,1-Diphenylpropargyl Alcohol to a Hydroxybenzocyclobutene and Related Reactions. *Inorganics* **2017**, *5*, 80.

(41) (a) Seiller, B.; Bruneau, C.; Dixneuf, P. H. Novel Ruthenium-catalysed Synthesis of Furan Derivatives via Intramolecular Cyclization of Hydroxy Enynes. *J. Chem. Soc. Chem. Commun.* **1994**, *2*, 493–494. (b) Liu, Y.; Song, F.; Song, Z.; Liu, M.; Yan, B. Gold-Catalyzed Cyclization of (*Z*)-2-En-4-yn-1-ols: Highly Efficient Synthesis of Fully Substituted Dihydrofurans and Furans. *Org. Lett.* **2005**, *7*, 5409–5412. (c) Du, X.; Song, F.; Lu, Y.; Chen, H.; Liu, Y. A general and efficient synthesis of substituted furans and dihydrofurans via gold-catalyzed cyclization of (*Z*)-2-en-4-yn-1-ols. *Tetrahedron* **2009**, *65*, 1839–1845.

(42) Buil, M. L.; Collado, A.; Esteruelas, M. A.; Gómez-Gallego, M.; Izquierdo, S.; Nicasio, A. I.; Oñate, E.; Sierra, M. A. Preparation and Degradation of Rhodium and Iridium Diolefin Catalysts for the Acceptorless and Base-Free Dehydrogenation of Secondary Alcohols. *Organometallics* **2021**, *40*, 989–1003.

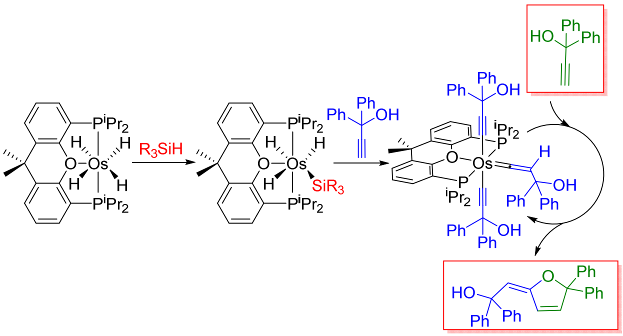

R3SiH